Rare earth elements in Andaman Island surface seawater: Geochemical tracers for the monsoon?

Ed C. Hathorne[1*], Martin Frank[1], PM Mohan[2]

[1]GEOMAR Helmholtz Center for Ocean Research Kiel, Germany, [2]Department of Ocean Studies and Marine Biology, Port Blair, Pondicherry University, India

Submitted to Journal:
Frontiers in Marine Science

Specialty Section:
Marine Biogeochemistry

Article type:
Original Research Article

Manuscript ID:
440330

Received on:
01 Dec 2018

Revised on:
13 Nov 2019

Frontiers website link:
www.frontiersin.org

Conflict of interest statement

The authors declare that the research was conducted in the absence of any commercial or financial relationships that could be construed as a potential conflict of interest

Author contribution statement

EH and PMM collected the samples. EH performed the analyses and wrote the manuscript with contributions from MF and PMM.

Keywords

yttrium and lanthanides, Bay of Bengal (BoB), Andaman Island, Nd isotope composition, River seasonality

Abstract

Word count: 347

The Asian summer monsoon affects the lives of billions of people. With the aim of identifying geochemical tracers for the monsoon related freshwater input from the major rivers draining into the Bay of Bengal and the Andaman Sea we have taken surface seawater samples from various locations spanning the Andaman Islands in 2011 to 2013. In some locations, samples have been taken in March, July and November 2011 thus spanning the seasonal cycle and including different monsoon phases. Generally, the YREE patterns are similar to those reported for offshore samples from the Bay of Bengal and Andaman Sea in January 1997 with seawater normalised REE patterns of most samples are characterised by middle REE enrichments. An enhancement of these middle REE bulges accompany large increases in dissolved REE concentrations from streams and sediment rich areas such as mangrove environments. Conversely, some samples, in particular those taken 1-2 days after heavy rainfall in March 2011, show pronounced REE scavenging accompanied by the preferential removal of dissolved light REEs and by higher Y/Ho ratios. The Nd isotope signature of the remaining dissolved REE phase of these low YREE samples is more radiogenic compared to local rocks and sediments.

The time series at a location away from local input sources shows remarkably similar REE patterns and concentrations in March and July. Then in October-November, following the peak in monsoon induced river discharge, the dissolved REE concentrations increase by almost a factor of 2 while Nd isotopes become less radiogenic by 1.5 εNd units. These unradiogenic values are found at the same site in the winter dry season of the following year demonstrating the decoupling of sea surface salinity and Nd. The large sub-annual variability of YREE concentrations and Nd isotopes encountered was likely caused by the conversion of YREE from the dissolved (probably colloidal) pool to the labile particulate fraction. The comparison of unfiltered and filtered sample concentrations reveals the existence of a large labile particulate pool in the BoB and AnS that most likely originates from the massive river sediment fluxes and is instrumental in the seasonal changes observed.

Ethics statements

(Authors are required to state the ethical considerations of their study in the manuscript, including for cases where the study was exempt from ethical approval procedures)

Does the study presented in the manuscript involve human or animal subjects: No

Data availability statement

Generated Statement: All datasets generated for this study are included in the manuscript and the supplementary files.

Rare earth elements in Andaman Island surface seawater: Geochemical tracers for the monsoon?

Ed C. Hathorne[1], Martin Frank[1], P.M. Mohan[2]
[1]GEOMAR Helmholtz Centre for Ocean Research Kiel, Wischhofstraße 1-3, Kiel, Germany, ehathorne@geomar.de
[2]Department of Ocean Studies and Marine Biology, Pondicherry University, Port Blair 744 103, Andaman & Nicobar Islands, India

Abstract

The Asian summer monsoon affects the lives of billions of people. With the aim of identifying geochemical tracers for the monsoon related freshwater input from the major rivers draining into the Bay of Bengal and the Andaman Sea we have taken surface seawater samples from various locations spanning the Andaman Islands in 2011 to 2013. In some locations, samples have been taken in March, July and November 2011 thus spanning the seasonal cycle and including different monsoon phases. Generally, the YREE patterns are similar to those reported for offshore samples from the Bay of Bengal and Andaman Sea in January 1997 with seawater normalised REE patterns of most samples are characterised by middle REE enrichments. An enhancement of these middle REE bulges accompany large increases in dissolved REE concentrations from streams and sediment rich areas such as mangrove environments. Conversely, some samples, in particular those taken 1-2 days after heavy rainfall in March 2011, show pronounced REE scavenging accompanied by the preferential removal of dissolved light REEs and by higher Y/Ho ratios. The Nd isotope signature of the remaining dissolved REE phase of these low YREE samples is more radiogenic compared to local rocks and sediments.
The time series at a location away from local input sources shows remarkably similar REE patterns and concentrations in March and July. Then in October-November, following the peak in monsoon induced river discharge, the dissolved REE concentrations increase by almost a factor of 2 while Nd isotopes become less radiogenic by 1.5 εNd units. These unradiogenic values are found at the same site in the winter dry season of the following year demonstrating the decoupling of sea surface salinity and Nd. The large sub-annual variability of YREE concentrations and Nd isotopes encountered was likely caused by the conversion of YREE from the dissolved (probably colloidal) pool to the labile particulate fraction. The comparison of unfiltered and filtered sample concentrations reveals the existence of a large labile particulate pool in the BoB and AnS that most likely originates from the massive river sediment fluxes and is instrumental in the seasonal changes observed.

INTRODUCTION

The rare earth elements (REEs) have been recognised as a means to detect trace metal input from rivers to coastal waters since the pioneering work of Elderfield and colleagues in the 1980s (Hoyle et al 1984; Sholkovitz and Elderfield, 1988, Goldstein and Jacobsen 1988 a; Elderfield et al. 1990). Examining the relative concentrations of

some or all of the 14 naturally occurring REEs and yttrium provides a wealth of information as fractionation amongst this chemically coherent group of elements reflects solution speciation, particle exchange processes, source oxidation state and the preferential incorporation into and subsequent release from different minerals (e.g. Cantrell & Byrne, 1987; Byrne et al., 1991; Moffett, 1994; Bau 1999; Hannigan and Sholkovitz, 2001; Quinn et al., 2006, and see Elderfield 1988 for a review that still remains insightful and relevant after 30 years). Even more information can be gleaned from the radiogenic isotope composition of the light REE neodymium as ^{143}Nd is the alpha decay product of ^{147}Sm and hence the $^{143}Nd/^{144}Nd$ ratio (expressed relative to the initial bulk Earth composition called CHUR in epsilon units) reflects the type and age of rocks which impart their signature to rivers and seawater through weathering (e.g. Goldstein and Jacobsen 1987, 1988b; Bertram and Elderfield, 1993; Frank 2002; Lacan et al., 2012; van der Flierdt et al., 2016). Elderfield et al. (1990) suggested the relative REE concentrations or "REE pattern" of filtered river water is controlled by two pools; 1) the colloidal pool consisting of REE bound to small particles like Fe oxy-hydroxides or organic matter, and 2) the truly dissolved pool in which the REEs are bound to simple inorganic ligands like carbonate. The relative proportion of these pools is a function of river chemistry including organic and inorganic ligand concentrations and pH (Tang and Johannesson, 2010). The importance of the colloidal pool is most obvious when river water first meets salty water in the estuary and salt induced coagulation removes most, if not all, of the REEs contained in the colloidal pool (e.g. Sholkovitz and Szymczak 2000). This results in a range of estuarine Nd removal from 97 to 40% (Rousseau et al., 2015 and references therein; Adebayo et al., 2018) and exerts a fundamental control on the REE signal of river input and the REE budget of the oceans. Experiments with filtered river and seawater suggest that much of the variability in estuarine removal is related to the character of the colloid fraction REE. Organic matter bound REE behaves nearly conservatively while waters rich in inorganic colloids quickly lose their REE load as salinity increases (Merschel et al., 2017a).

The South Asian Monsoon (SAM) affects the livelihoods of more than a billion people providing vital water resources on one hand and devastating floods and landslides on the other (Krishna Kumar et al., 2004; Gadgil and Gadgil 2006; Turner and Annamalai, 2012; Duncombe 2018). Four of Earth's great rivers; the Ganges (Ganga) and Brahamaputra (G-B), Irrawaddy (or Ayeyawady) and Salween (I-S) discharge more than 1000 $km^3\ yr^{-1}$ of freshwater (Dai et al. 2009) into the Bay of Bengal (BoB) and the Andaman Sea (AnS) (Figure 1). These monsoon fed rivers also deliver some of the highest sediment loads globally (Milliman and Syvitski, 1992), which has built the Bengal and Nicobar fan, the largest submarine fan system on Earth (Curray et al., 2002). The discharge of these monsoonal rivers is highly seasonal following spring snow melt and most importantly summer monsoon precipitation (Shaman et al., 2005; Jian et al., 2009). Large sub-seasonal and inter-annual variability of G-B discharge is tightly linked to monsoon precipitation peaking from June to October (Jian et al., 2009) and these variations impact BoB sea surface salinity (SSS). As such the BoB and AnS are characterized by a thin (<20 m) low salinity mixed layer persisting year round which is maintained by a roughly equal mixture of river discharge and direct

monsoon precipitation over the ocean and often displays two steps of increasing salinity with depth (Sengupta et al., 2006). The halocline below this fresh layer is normally shallower than the thermocline and the layer between them is referred to as the barrier layer (e.g. Girishkumar et al., 2011). This barrier layer has been implicated in cyclone intensification (Sengupta et al., 2006) and the thickness of the fresh mixed layer and barrier layer is driven by seasonally reversing winds and ocean currents with mesoscale eddies facilitating vertical mixing (Durand et al., 2011; Girishkumar et al., 2011, 2013; Akhil et al., 2014, 2016). Recent observations of SSS variability suggest this feature is dominated by the freshwater flux and not surface circulation (Chaitanya et al., 2015) although weakened currents resulting from Indian Ocean dipole modes may play a role in trapping freshwater in the BoB (Pant et al., 2015). Recent mooring observations in the northern BoB between the G-B and I river mouths demonstrate that SSS can drop by 4 psu units in 5 days as river discharge fronts pass (Sengupta et al., 2016). Despite recent advances in observational coverage of the region (e.g. Girishkumar et al., 2011), the hydrographic variability in areas like the AnS remains poorly understood (Chatterjee et al., 2012) and under sampled.

Amakawa et al. (2000) first reported elevated REE concentrations of BoB and AnS surface waters compared to the rest of the Indian Ocean with a distinctive REE pattern and unradiogenic Nd isotopes most likely reflecting the weathering input from South Asia. These elevated REE concentrations with a globally distinctive broad middle REE enrichment and similar normalised La and Lu values were found to extend to deeper BoB and AnS waters (Nozaki and Alibo, 2003). This most likely originates from the inputs of the great rivers but the dissolved river flux (estimated as very few dissolved river REE data exist for the region) is a factor of 10 too low leading Nozaki and Alibo, (2003) to suggest that the supply of excess BoB REEs could be accounted for by the dissolution of no more than 0.3% of the sediments brought by the rivers. More recent studies focusing on Nd isotopes and concentrations have revealed a substantial excess Nd concentration throughout the BoB, which has a calculated Nd isotope composition similar to modern G-B river sediments and suggests release from Bengal Fan sediments (Singh et al., 2012). The re-sampling of similar locations a few years later found significantly lower Nd concentrations and more radiogenic Nd isotope signatures leading to the suggestion that the Nd isotope composition of BoB seawater varies seasonally and inter-annually with river sediment discharge (Yu et al., 2017a). Furthermore, these authors presented Y and REE data for their BoB samples which suggested that the freshwater input into the BoB can be traced with YREE ratios (Yu et al., 2017b). Such variability is hard to reconcile with the Nd oceanic residence time on the order of centuries (e.g. Tachikawa et al., 1999) and the calculated YREE residence times for BoB surface water (Yu et al., 2017b). Despite these clear signals, it was not possible to conclude if the variability observed between these studies was truly seasonal/inter-annual or resulted from spatial heterogeneity (Yu et al., 2017a). If these potential proxies for river discharge into the BoB and AnS are to be used for filling the large data gaps in this region, the seasonal fluctuation of the REE concentrations and signatures needs to be verified with a stationary time series and suitable archives for past REE variations need to be identified.

Despite a compelling consensus that the vast majority of REE associated with planktonic foraminifera shells is acquired at the sea floor from bottom waters or porewaters during early diagenesis (Roberts et al., 2010, 2012, Tachikawa et al., 2013; Kraft et al., 2013; Osborne et al., 2017; Skinner et al., 2019), some workers have used the Nd/Ca of planktonic foraminifera shells to infer past changes in monsoon induced run-off (Liu et al., 2015; Nilsson-Kerr et al., 2019). However, while the annual density bands of massive coral skeletons are a promising recorder of mixed layer seawater REE concentrations (e.g. Wyndham et al., 2004; Saha et al., 2016), the processes controlling the YREE concentrations and Nd isotope signatures of seawater within and around the coral reef system need to be understood before such proxies can be reliably applied in the past. With this goal in mind we have systematically sampled surface seawater from around coral reefs of the Andaman Islands which form the geographic boundary between the BoB and AnS. These data demonstrate that seawater REE concentrations in the BoB do vary seasonally with the monsoon induced river water discharge. However, we also identify many local processes that can modify the YREE and Nd isotope signal on short time and length scales meaning coral REE signatures from such settings must be interpreted with caution.

METHODS

Study Area

The Andaman Islands are situated some 600 km west of Thailand and 1300 km east of mainland India and extend from around 10°N to 14°N (Figure 1). Formed by the uplift of the accretionary prism of the Sunda Trench the Andaman Islands are composed of sedimentary rocks of late Cretaceous to Miocene age sitting on top of ophiolitic volcanics and basalts (Allen et al., 2008a; Garzanti et al., 2013). Barren Island to the east of the other islands is the only active volcano representing the active arc. Arc materials are present throughout much of the turbiditic mudrocks and sandstones of the Andaman Flysch and Mithakhari Group (Allen et al., 2008a) and it is these Paleogene rocks that are most exposed on the main three islands of South, Middle and North Andaman (Garzanti et al., 2013) (Figure 2). These sedimentary rocks represent the erosional product of the Himalayan orogeny delivered mostly by the Irrawaddy river (Garzanti et al., 2013) and sediments with similar composition and zircon ages extend from the Indo-Burman ranges in the north (Allen et al., 2008b) to the Nicobar fan in the south (McNeill et al. 2017). On the smaller surrounding islands, where coral reefs are abundant, are exposures of the Neogene Archipelago group which contain sandstones, chalk and limestones (Allen et al., 2008a) deposited on the slope (Pal et al., 2005). The summer monsoon rains usually begin in May on the Andaman Islands, earlier than mainland India (Fasullo and Webster 2003), and the high precipitation season is normally at full strength by early July (Figure 3). Being sparsely populated, with most development centred around the capital Port Blair, the Andaman Islands are mostly undisturbed and covered by dense rain forest that extends to the beach and the coral reefs. In low lying areas mangrove forests and glades are found next to the reefs. As such they present an increasingly rare opportunity to study the geochemistry

of virtually undisturbed reef ecosystems. Unfortunately these islands are not immune from global change and substantial coral bleaching (Sarkar and Ghosh, 2013).

Regrettably the oceanography of the AnS is very poorly studied and even today relatively few Argo floats make it there to improve this dearth of knowledge (e.g. Thadathil et al., 2007). Even less is known about the oceanography around the Andaman Islands. The water chemistry around the islands is likely driven by the monsoon rains, river discharge and seasonally reversing ocean currents (Chatterjee et al., 2017). The AnS is open to surface water exchange with the BoB at the Prepairs Channel between North Andaman Island and the Ayeyawady (Irrawaddy) delta in Myanmar, while the 10 Degrees Channel between Little Andaman and Great Nicobar Islands and the Great (or 6 Degree) Channel between the Nicobar Islands and Sumatra provide deeper connections. Generally it is thought that the surface circulation in the AnS is cyclonic during the SW monsoon and the reverse during the NE monsoon (Varkey et al., 1996) but more modern analyses suggest the situation is more complex with a mean flow towards the SE in summer and towards the SW in winter (Rizal et al., 2012). Forced by both remote equatorial Wyrtki jets and local winds, strong surface currents probably form along the Islands during the monsoon transitions in spring and autumn (Chatterjee et al., 2017). Much of the large monsoonal sediment flux from the nearby Ayeyawady (Irrawaddy) and Salween rivers is trapped in the Gulf of Martaban (Ramaswamy et al., 2004) but the surface waters of the reefs become noticeably turbid during the summer monsoon season. The study of recent sediments from the north eastern BoB and AnS indicates that the small Arakan coast rivers supply a disproportionally large fraction of terrigenous sediments with radiogenic Nd isotope signatures to the region (Colin et al., 1999; Damodararao et al., 2016).

Sample collection and processing

Surface samples were collected in PE bottles while swimming or from the side of small wooden boats (no deeper than an arms length) from open ocean locations with extensive coral reefs and more inshore locations (see Supplementary Figure 1 for an example). In a few instances a small Niskin bottle on a rope was employed. Fresh water samples were collected by holding the PE bottle in the stream or waterfall. All samples were filtered within a few hours at 0.22 or 0.45 microns (cellulose acetate membranes) using the vacuum produced by a water jet and a Nalgene PC 42mm diameter filter holding device. This was rinsed with >18.2 MΩ water between samples and the first approx. 500mL of filtered sample was discarded. During the first sampling campaign an unfiltered sample aliquot was also kept for some selected samples. In all subsequent sampling an unfiltered sample aliquot was kept for all samples, with the exception of the large volume samples which were limited in number by logistical reasons. The large volume samples for Nd isotope analyses were obtained by filling two 20L collapsible cubic containers as much as possible while snorkleling or from the side of a wooden boat. These where then filtered directly after collection using a hand operated peristaltic pump and a 142 mm diameter filter holder with 0.45 micron cellulose nitrate filter membranes into a acid cleaned 20L col-

lapsible cubic container. The cubic containers used for sample collection where rinsed with 10% HCl (analytical grade) and >18.2 MΩ water (Milli-Q) before the next use. During collection the cubic containers were first rinsed with sample before the sample was taken. Particularly sediment rich samples required the use of multiple membranes. Filtered and unfiltered samples (125 mL) were acidified to pH 2 in the field using distilled HCl prepared in the clean labs at GEOMAR, Germany. A small aliquot of filtered sample was filled into a 1.4 mL glass vial with no head space and sealed with a septum lid and Parafilm™ for stable isotope and chloride analyses.

Salinity was measured in the field to 0.1 psu during sample collection and after filtering using a hand held conductivity sensor made for domestic aquarium purposes. This was cross calibrated with a WTD conductivity sensor and gravimetrically prepared NaCl solutions before going into the field.

Jolly Bouy Island was sampled in 2011 and both February and March 2012, and again in March 2013. A few key locations distributed along the islands have been resampled in March 2013.

Rain water samples were obtained in January 2015 from the deck of the JOIDES Resolution drill ship while operating near Little Andaman Island. Rain was collected in an acid cleaned PE beaker and filtered through a 0.2 µm polysulfone disc filter with an acid cleaned syringe directly after collection. The filtered rain samples were acidified to 1% by volume with Seastar grade HNO_3.

In the laboratory at Pondicherry University in Port Blair FeCl solution (purified in the GEOMAR laboratory) was added to the 20L volume samples for Nd isotope analysis and allowed to equilibrate for 24-48 hours. After equilibration the pH was raised to 7.5 to 8 by the step wise addition of Merck Suprapur grade (imported by Sigma-Aldrich India) ammonia solution. The resulting FeOH precipitate was allowed to settle for 24-48 hours before the excess seawater was siphoned off and only the FeOH precipitate was taken to Germany. Back in the laboratory at GEOMAR the FeOH precipitate was further concentrated, dissolved and excess Fe removed by an ether back extraction before Nd was purified using routine techniques in our laboratory (Stichel et al., 2012) producing yields of approximately 70%.

Analytical Methods

Salinity and $\delta^{18}O$ - $\delta^{2}H$

Samples were analyzed for $\delta^{18}O$ and $\delta^{2}H$ by isotope ratio infrared spectroscopy (L 1102-i WS-CRDS, Picarro Inc., Santa Clara, CA, USA) at the Friedrich-Alexander University Erlangen-Nürnberg, Germany. All values are reported in the standard δ-notation (‰) vs. VSMOW and external reproducibility based on repeated analyses of a control sample was better than 0.1‰ and 0.5‰ (±1 sigma) for $\delta^{18}O$ and $\delta^{2}H$, respectively. A detailed description of the analytical procedure used is given in van Geldern and Barth (2012). Following stable isotope analyses the chloride concentra-

tion of the samples was determined by titration with silver nitrate using a METROHM auto-titrator. IAPSO standard seawater (Cl = 19.376 g/kg or as specified on the bottle; the sum of chloride and bromide is 559 mM) was used to calibrate the results and the precision is estimated to be 0.3% based on repeated measurements of IAPSO.

Yttrium and REE

Analysis of the YREE concentration of most of the samples was performed using a seaFAST online preconcentration (OP) system coupled to an Agilent 7500ce ICP-MS as described in Hathorne et al. (2012). This method was part of the GEOTRACES intercalibration exercise (van de Flierdt et al., 2012) and has been demonstrated to produce accurate Nd concentrations compared to isotope dilution measurements of the same samples on numerous occasions (Hathorne et al., 2012; Grasse et al., 2017; Laukert et al., 2017). The long term average values obtained for the Bermuda Atlantic Time-Series (BATS) 15m and 2000m samples, during the course of this study are presented in Table S1.

YREE data obtained for the March 2013 samples utilised a newer syringe pump type seaFAST instrument (SV400) coupled with a Thermo Fisher Element XR SF-ICP-MS. These measurements employed a 4mL loop and the instrument was run in low resolution and scan speed optimisation mode to obtain time resolved data. Such time resolved analysis has been found to improve precision for such low volume analyses (Osborne et al., 2015). Calibration curves for these measurements were obtained by standard additions of a mixed YREE solution with a seawater like pattern to a large volume surface seawater sample from the South Atlantic. The average values obtained for the 15m BATS reference seawaters during these analyses and a reference seawater from the Cape Basin "CAB" are also presented in Table S1.

Unfiltered samples were first centrifuged at 3500 rpm (Eppendorf 5810 max 2900 times g) for 30 mins before the supernatant was transferred to a fresh tube for analysis. The filtered sample concentrations are operationally defined as "dissolved" while the unfiltered samples represent both the dissolved and the weak HCL soluble pool referred to here as "easily exchangeable" or labile.

Procedural blanks taken in the field (n = 5) by filtering >18.2 MOhm water acidifying and storing with the samples were also analysed by OP-ICP-MS with the samples. Repeated analyses of these blanks in the most recent analytical session reveals they are <0.5 pmol/kg for the LREE to below detection limits (e.g. <0.03 pmol/kg Lu) for the HREE. For the LREE this is 20% for the anomalously low concentration samples but only on the order of 1% for LREE in the vast majority of samples and is also negligible for the MREE and HREE (including Y).

Neodymium isotope measurements were performed with either a Nu instruments MC-ICP-MS at GEOMAR or a Thermo Fisher Neptune Plus MC-ICP-MS at the ICBM, University of Oldenburg, Germany. Solutions with concentrations from 5ppb and higher were measured and values were normalised to the accepted $^{143}Nd/^{144}Nd$ of the JNdi-1 isotope standard of 0.512115 (Tanaka et al., 2000). Based on repeated meas-

urements of the JNdi-1 and an in-house Nd standard "Merck" from the ICBM the 2s external precision of the measurements expressed as εNd is 0.4 units. Repeated measurement of one sample with a high Nd concentration (AN12) on both instruments gave a comparable precision of 0.4 epsilon units.

RESULTS

The field measured salinities and those determined later by silver nitrate titration generally agree very well (slope of 0.98 with a zero intercept $R^2 = 0.94$).
Freshwater samples (apart from the rain) plot on the global $\delta^{18}O$ vs $\delta^{2}H$ meteoric water line and the other samples generally form a mixing line between the seawater and freshwater (Supplementary Figure 2). A few samples deviated from this relationship suggesting that evaporation may have occurred since collection. The $\delta^{18}O$, $\delta^{2}H$, and salinity data for these samples were excluded and are not reported or discussed.

GEOGRAPHICAL VARIABILITY

Salinity varies widely and this patchiness is also clear in the high resolution World Ocean Atlas climatology shown here for November (Figure 1) and in recently acquired field data (Kiran Kumar et al., 2018). Away from river or stream mouths the salinity ranged from 34 to 31 over our sampling period with the freshest values found on the AnS side of the Islands during November 2011 (Figure 2). Some of the variability of salinity observed across the islands is also likely to be temporal as these locations were sampled over a few weeks during each sampling campaign. March 2011 was particularly wet with anomalously high rainfall on the Andaman Islands (Figure 3). NE Interview Island showed the saltiest waters both in March 2011 and 2013 (Figure 2). This suggests that either surface circulation brought more saline waters to this northerly exposed location or there was supply from a local source of saltier water, perhaps a very shallow lagoon nearby formed by uplifted coral reefs.

The concentration of REEs in the filtered seawater samples varied greatly with Nd ranging from 1.6 to 120 pmol/kg while Yb concentrations varied from 2.15 to 20.5 pmol/kg (shown as shale normalised values in Figure 4, Table S1). The lowest concentrations were encountered after a rain event in March 2011 (Figure 3) and consistently at one beach location on Neil (Shaheed Dweep) Island in both 2011 and 2013 (Figure 4 samples AN48, AN54, AN124). The highest concentrations are from locations inland up tidal creeks (Figure 4 samples AN13, AN140) or next to small river mouths where the sediment loading was high (Figure 4 samples AN88, AN146). Shale normalised patterns (Figure 4) broadly resemble seawater from other locations including a HREE enrichment and relatively depleted Ce concentrations (negative Ce anomaly) but in some samples a MREE enrichment is clearly evident. There is no simple relationship between salinity and YREE concentrations except for the few filtered samples with salinities less than 31.5 which display a clear negative relationship, especially for the HREE. However, the vast majority of samples with salinities >31.5 have higher YREE concentrations.

Filtered freshwater concentrations range from 26 to 277 pmol/kg Nd and 3.3 to 25 pmol/kg Yb. Concentrations in the filtered rainwaters are low but substantial with Nd ranging from 1.4 to 4.5 pmol/kg while Yb concentrations range from 0.2 to 0.7 pmol/kg. Shale normalised patterns for the freshwaters either display strong MREE enrichments or more seawater like patterns with enhanced HREE concentrations (Figure 5).

The concentrations encountered in the unfiltered samples represent the particulate YREE that are leachable in 0.1% HCl over months to years, as well as the dissolved YREE. This ranges from values similar to filtered samples to extremes of 780 pmol/kg Nd and 141 pmol/kg Yb. For example, samples from Jolly Buoy Island exhibit very little difference (unfiltered/filtered near 1) whereas some of the stream and river mouth samples have the highest easily exchangeable YREE concentrations (unfiltered/filtered > 10).

TEMPORAL VARIABILITY

At three readily accessible locations, Smith Island, Avis Island and Jolly Buoy Island, we were able to obtain multi-season and in some cases multi-year time series. Both Smith and Avis island time series reveal anomalously low YREE concentrations 1-2 days after a sustained 2 day rain event in March 2011 (Figure 6) while the salinity was only significantly lower at Avis island in July and both Avis and Smith islands in November. The Avis Island time series exhibits a large range of concentrations similar to that encountered in all other samples, but at one single location, where very high concentrations (83 pmol/kg Nd) occurred during the monsoon in July 2011 (Figure 6). At Jolly Buoy island the range in concentrations is smaller and the maximum concentrations occurred later in the year in November (Figure 7). Between March and November the salinity at Jolly Buoy Island decreased by 1 psu and the Nd (YREE) concentration peaks but decreased again while salinity remained low (Figure 8). A similar relationship between Nd concentrations and salinity in the inter-annual samples is not observed.

NEODYMIUM ISOTOPES

A wide range of Nd isotope values are encountered in the filtered samples, from -9.6 to -2.6, with an apparent relationship with Nd concentrations (Figure 9). The Nd isotope composition at the Jolly Buoy site was -7.6 in March 2011 and then an invariable signature of -9 in November 2011 and February and March 2012 (Figure 8). This consistency is in strong contrast to the variations in salinity and Nd concentration between these sampling periods. The other sample from the western, BoB side of the Islands (Interview Island) also has a similar Nd isotope composition while samples from the eastern side of the Islands in the AnS have more radiogenic values ranging from -7 to -2.6. The most radiogenic values were measured for the samples with lowest Nd and YREE concentrations (Figure 9).

DISCUSSION

Local sources of YREE to seawater

The dissolved Nd isotope composition measured is overall consistent with the local and regional geology (Figure 9) although the more radiogenic values were measured in clay size separates from the Archipelago group and from Karmatang beach (Ali et al., 2015) which may represent a mixture of source rock contributions from the ophiolite and Mithakhari Melange (Garzanti et al., 2013). However, these rocks will only be of local importance and the widespread enrichment of surface waters in Nd, evident also far away from the islands (Amakawa et al., 2000, Nozaki and Alibo, 2003), suggests that most of the radiogenic Nd likely originates from the Irrawaddy or Indo-Burman Ranges (IBR) rivers (Allen et al., 2008b), especially in November. Like all samples from the BoB measured so far, the surface waters of the Andaman Islands exhibit a pronounced enrichment of the MREE relative to other ocean regions (Figure 10). A MREE enrichment has been found in many rivers (e.g. Elderfield et al., 1990; Sholkovitz, 1995) and has been attributed to phosphate mineral weathering (Hannigan and Sholkovitz, 2001), release from iron oxides/hydroxides (Tang and Johannesson, 2010) or possibly from sedimentary organic matter (Freslon et al., 2014). The carrier of the MREE enrichment is likely present in the colloidal phase as it is not observed in the truly dissolved measurements of the Amazon tributary Solimões which drains the Andes and is rich in inorganic colloids (Merschel et al., 2017b). A MREE bulge is also observed in the Yamuna tributary of the Ganga and local Andaman Island streams Jonga Nallah and Saddle Peak (Figure 5). The Saddle Peak stream samples ophiolite rocks while the Junga Nallah source (AN92) is located on the Mithakhari Melange (Garzanti et al., 2013). The other streams sampled exhibit seawater like REE patterns like observed for rivers with higher pH values such as the Mississippi (e.g. Shiller 2002, Adebayo et al., 2018), although with strong variations in concentrations. The stream on Interview Island flows through the carbonate rich Archipelago group and has relatively high YREE concentrations. The waterfall sampled on Little Andaman Island most likely flows across the Archipelago group with Miocene limestones (Sarkar and Ghosh, 2015), and has the lowest stream REE concentrations. Interestingly, the S Andaman Island stream near the east coast flows over the ophiolite rocks (Allen et al. 2008a) but has REE concentrations intermediate between Interview Is. and Little Andaman Is. streams with LREEs similar to Little Andaman and HREEs similar to Interview Is. All this suggests that the local geology is not the only factor controlling the REE concentrations in the streams.

The potential of local streams to influence the surface seawater YREE pattern will depend on the removal of YREE during mixing with seawater and salt induced coagulation and the transfer of colloidal bound YREE to particles and their subsequent re-release from sediments (e.g. Elderfield et al., 1990; Sholkovitz and Szymczak, 2000; Rousseau et al., 2015; Adebayo et al., 2018). The few brackish water samples taken at the stream mixing zones suggest <50% removal (the difference between the freshwater and brackish sample pair) of LREEs and virtually no removal for the HREE (Table S1). Such limited removal is less than the global river average of 70% (See Rousseau et al. 2015 and references therein) but similar results have been found for the Mississippi river and may be attributable to the relatively low YREE concentrations in the

river water (Adebayo et al., 2018). Besides the Jonga Nallah and Interview Island samples, the stream water concentrations are of a similar magnitude to the highest seawater samples (Figures 4 & 5). The highest concentrations are from locations inland up tidal creeks surrounded by mangroves (Figure 4 samples AN13, AN140) or at small river mouths where the sediment loading is high (Figure 4 samples AN88, AN-146). Most importantly these samples have MREE bulges like observed in many of the samples (Figure 10). However, this MREE bulge pattern is found throughout the AnS and BoB and may originate from both local input or from the great rivers to the north (Figure 5).

The dust flux in the BoB exhibits a strong gradient from 0.3 to 6 g/m2/yr decreasing to the south and east and varies seasonally (Srinivas and Sarin, 2013). This large range is similar to that generally encountered in the northern hemisphere oceans (with the exception of the extremes of the tropical N Atlantic and Arabian Seas; Mahowald et al., 2005) and is similar to the lithogenic flux measured in southern BoB sediment traps (Unger et al. 2003), suggesting that dust could possibly be a source of YREE to surface seawater. However, the rain samples collected during the NE winter monsoon when winds may have supplied dust from the Asian continent have very low YREE concentrations and indicate atmospheric sources of dissolved YREE are likely insignificant (Figure 5). The concentrations measured in the Andaman Sea rain samples are low compared to those found in the N Atlantic (Sholkovitz et al., 1993) and W Pacific (Nozaki et al., 1997). Although the concentrations measured in the filtered Andaman Sea rainwater (average of 3 pmol/kg Nd) are much lower than concentrations observed in the Western Pacific (filtered values from 11.8 to 40.9 pmol/kg Nd) by Nozaki et al., (1997) the shale normalised patterns are similar being relatively flat from La to Lu.

All this suggests that local inputs are clearly important to more inland samples and immediately at the mouths of streams whereas the vast majority of the samples from around the reefs and outer islands reflect a more regional source of REE.

Rapid removal of dissolved YREE

The highly radiogenic values encountered following the removal of much of the Nd from the dissolved phase during the March 2011 rain event, suggest that the remaining Nd was sourced from more mantle derived radiogenic rock formations. The REEs remaining in solution have a similar concentration and shale normalised pattern (Figure 11) to the ultra-filtered measurements of the truly dissolved fraction in the Amazon tributary Solimões (Merschel et al., 2017b). It also is interesting to note that the truly dissolved Solimões sample is some 2 εNd units more radiogenic than the >1kDa fraction (Merschel et al., 2017b), consistent with the radiogenic nature of the low REE samples observed here. Although a very general comparison made necessary by the scarcity of ultra-filtered water data, this suggests that the remaining REEs may represent the truly dissolved fraction characterised by a radiogenic Nd isotope composition. The rain sample (from a different place and time) has a Nd concentration similarly low to seawater after the rain event. However, the YREE patterns of the rain

and the YREE depleted surface water are distinctive and suggest that the rain was not a likely source for the highly radiogenic waters. Considering the likely dust sources to the region, Indian deserts with Himalayan derived sediments or even Asian loess (e.g. Srinivas and Sarin, 2013), have much less radiogenic Nd isotope signatures, the rain itself cannot be responsible for the low Nd concentrations with radiogenic signatures. The change in salinity observed after the rain event in March 2011 is also too small for any significant volume of rainwater to have mixed with the surface waters causing these radiogenic values. The comparison of concentrations in the unfiltered and filtered samples reveals that there is much more Nd in the leachable particulate phase than needed to offset the loss from the dissolved pool after the rain event. The highest unfiltered/filtered values of 100 (see discussion below) were found for these samples with active removal of YREE from the dissolved phase (e.g. AN11, AN14, AN17, AN124) which have more extreme LREE enriched unfiltered/filtered patterns compared to those samples whose unfiltered/filtered ratio is high because they were taken at stream or river mouths or inshore locations (e.g. AN44, AN104, AN146). Importantly, these unfiltered samples have relatively high concentrations suggesting the active conversion from the colloidal fraction to the labile particulate pool (Figure 12). Additionally, the concentrations in these unfiltered samples are many times higher than the amount of REE removed following the rain event (e.g. 84 versus 7 pmol/kg at Smith Island) and also much higher than observed in unfiltered samples at the same location during later visits (Figure 12). The shale- normalised pattern of these unfiltered samples does not suggest the presence of fresh volcanic material (Figure 12) that would help to explain the radiogenic Nd isotope values encountered in the filtered seawater but not the low dissolved YREE concentrations. Instead the unfiltered YREE patterns suggest the input of locally derived suspended particulates (compare to inland sample AN12 unfiltered in Figure 12) as a result of the rain event, which then removed the colloidal component of the seawater. This could potentially occur by two ways; 1) the fresh local particles, not being equilibrated with seawater, could attract nearby colloids and/or simply collect colloids that they collide with, or 2) transported in a thin layer of freshwater runoff, the fresh particles and freshwater are mixed with the underlying seawater and colloidal flocculation mimicking estuarine mixing occurs on small length scales. It could also be the case that addition of dissolved Fe in the runoff would promote Fe hydroxide precipitation once mixed with seawater. It is informative to note that similarly low dissolved YREE concentrations associated with a high labile particulate fraction was also found for samples from the western (sun set) beach on Niel (Shaheed Dweep) Island (Figure 12). Variable salinity at the beach during sampling may be indicative of some groundwater discharge component, which may have introduced some particles that enhanced the removal of YREE from the dissolved pool or seawater recirculating through the aquifer encounters freshwater and colloidal flocculation occurs. This feature was persistent at this location over all sampling visits and should be the focus of future work. More ultrafiltration work on river, seawater and groundwater samples is required to confirm these suggestions but the fortuitous sampling achieved here demonstrates that migration of YREEs from the dissolved pool to the labile particulate pool occurs on the timescale of days (Figure 6).

LABILE PARTICULATE YREE

The leachable (0.1% HCl by volume making the pH around 2) particulate concentrations of Al, Fe and Mn obtained in a similar manner to here from unfiltered samples from the shelf off South Georgia Island have been shown to correspond to particulate concentrations obtained from filters (Schlosser et al., 2018). Those samples from the Southern Ocean displayed high unfiltered/filtered concentration ratios for Fe and Al, but not for Mn, and direct comparison with particulate data indicates a fraction of the particulate Al and Fe was not leached from the particles in the unfiltered seawater (Schlosser et al., 2018). This suggests that the YREE concentrations measured in the unfiltered acidified seawater represent the labile particulate pool. The comparison of filtered and unfiltered samples reveals a very large readily exchangeable (in weak HCl) pool of suspended particulate YREE around the islands. Unfiltered/filtered values of up to 100 for Nd and many samples with values >10 are in stark contrast to studies of open ocean waters where labile particulate YREE is around 5% of the dissolved pool (unfiltered/filtered values around 1.05; Sholkovitz et al., 1994; Alibo and Nozaki, 1999). The highest unfiltered/filtered values observed here are on the order of 100 and are from the samples with anomalously low REE concentrations resulting from active removal of YREE from the dissolved phase (Figure 112; AN11, AN14, AN17, AN124). These have more extreme LREE enriched unfiltered/filtered patterns compared to those samples whose unfiltered/filtered ratio is high because of being close to local river or sediment input (Figure 12; AN104, AN146). The samples with high to intermediate YREE concentrations exhibit unfiltered/filtered values generally between 2 and 20 demonstrating the persistence of a large labile particulate fraction in the region. Many of the unfiltered/filtered patterns display a clear Y/Ho fractionation with Y being less enriched in the labile particulate fraction compared to Ho (Figure 12). This is to be expected as Y is less particle reactive than Ho despite having very similar ionic radii and charge (e.g. Bau, 1996; Nozaki et al., 1997). Both filtered and unfiltered samples from some stream waters and inland creeks with active input exhibit near crustal Y/Ho (PAAS has a molar Y/Ho of 50) with molar ratios around 60. However, for many sample pairs the Y/Ho ratio of the filtered sample is higher, around 80, and the most extreme examples being the samples with anomalously low filtered YREE concentrations having molar Y/Ho ratios around 100 while the labile particulate fraction has shale like ratios around 50 (Table S1) which have also been observed for Ayeyawady (Irrawaddy) shelf sediments (Kurian et al., 2008). These observations illustrate the control that the large labile particulate fraction has on the dissolved YREE patterns while indicating the dominance of crustal YREE in this fraction.

YREE CONCENTRATIONS AS TRACERS OF RIVER DISCHARGE

The elevated surface water YREE concentrations in the BoB have been taken as evidence for discharge of YREE from the great rivers draining into the Bay (Amakawa et al., 2000; Singh et al., 2012; Yu et al. 2017b). Based on N-S gradients in YREE concentrations in the BoB, Yu et al. (2017b) suggested high MREE* (MREE anomaly or bulge index) and low crustal Y/Ho ratios as good tracers for G-B river input but we have found similar patterns from local input from Andaman sediments. However, the

high MREE* values >2 observed in some Andaman stream samples are significantly eroded during stream mixing and there is no clear relationship between MREE* and salinity. The dissolved YREE concentrations from the Yamuna tributary of the Ganga, some 500 pmol/kg Nd, are high compared to Andaman streams (Figure 5) but the removal in the G-B, Irrawaddy and Salween estuaries is unknown and the removal upon mixing of Andaman streams appears relatively low (only 50%). Therefore it is not surprising that in many locations it seems that the local input of YREE, from runoff directly or released from particles and sediments, produces the dominant signal in surface water concentrations. This is evident in both Smith and Avis island time series where there are distinctive peaks in YREE concentrations (with high MREE* and low Y/Ho) in the July samples exhibiting low salinities with the local monsoon rains (compare July and November samples in Figure 6). Additionally, strong monsoon winds may lead to enhance sediment resuspension and YREE release. This contrasts with the Jolly Buoy time series where the YREE pattern remains similar throughout the year while YREE concentrations peak not in July following local monsoon rains but in November when the monsoon induced river discharge would most likely pass the islands (Jian et al., 2009). It seems that the relatively remote location of Jolly Buoy island, on the BoB side away from the larger islands and sediment sources (Figure 2), is the likely reason for the different timing of the YREE concentration peak. The Jolly Buoy samples also exhibit some of the smallest labile particulate YREE fractions measured here (Figure 12: plain circles), with the notable exception being the March 2011 sample (AN15), suggesting the labile particulate pool here is not sourced from discharge from the great rivers. Additionally, the samples from November with the highest YREE concentrations have very similar Y/Ho ratios to samples from the other seasons and the labile particulate pool has a slightly higher Y/Ho, strongly arguing against a fresh crustal source. At the same time the Jolly Buoy Island samples have relatively flat Andaman Sea Surface Water (ASSW PA-10 from Nozaki and Alibo, 2003) normalised patterns (Figure 11) suggesting these samples are representative of the wider region. The positive Indian Ocean dipole event of 2011 and 2012 led to strong freshening events in the BoB from rainfall (Pant et al., 2015) but importantly not river discharge. It maybe, therefore, that our sampling missed a large river discharge event and the associated YREE signal. Instead, exceptional rainfall in March 2011 appears to have generated the most distinctive YREE and Nd isotope signal in our dataset through the rapid migration of YREE from the dissolved to the labile particulate pool.

While the YREE distributions are clearly sensitive to interaction with particles the Nd isotope signatures of seawater are considered a more conservative tracer of input sources. As such we compare the εNd with YREE indices of BoB surface waters from this study and the literature (Amakawa et al. 2000; Yu et al., 2017a,b). The YREE indices suggested as being good potential proxies for G-B sediment input, namely Y/Ho and MREE* (Yu et al., 2017a), exhibit relatively little variability and no consistent relationship with εNd while the La/Yb molar ratio and the PAAS normalised Yb/Nd (referred to as HREE/LREE in Yu et al., 2017a) show a clear relationship with εNd (Figure 13). The one inshore sample influenced by local sediments (AN12 and marked in Figure 9) does not fit with the other data, again demonstrating that the εNd

of the other Andaman surface seawater samples likely reflects a regional signal. The close relationship between La/Yb and εNd suggests this can also be used to trace this regional signal.

Seasonal changes of Neodymium isotopes

Recent studies of Nd isotopes and concentrations in the BoB have revealed a substantial excess of Nd throughout the BoB when compared to the rest of the Indian Ocean and this excess has a calculated Nd isotope composition similar to modern G-B river sediments (Singh et al., 2012). The re-sampling of similar locations (Figure 1) a couple of years later found significantly lower Nd concentrations and more radiogenic Nd isotope signatures (Yu et al., 2017a). These authors thought this difference is most likely explained by the Nd isotope composition of BoB seawater varying seasonally and inter-annually with sediment discharge from the G-B river system (Yu et al., 2017a). However, as the samples were not taken at exactly the same location it was not possible to conclusively distinguish if the variability observed between these studies was truly seasonal/inter-annual or resulted from spatial heterogeneity (Yu et al., 2017a). Here we have shown with samples collected at three fixed locations over a year, that indeed the Nd isotope composition of filtered seawater can change on sub-annual timescales (Figures 6 & 9). We have compared the Nd isotope data from around the Andaman Islands with those from the surface (for this purpose we assume a mixed layer depth of 50 m) BoB from Singh et al. (2012), Yu et al., (2017a), and Amakawa et al. (2000) and a clear correlation between the Nd isotope composition and concentration appears (Figure 9). It must be noted that Amakawa and colleagues measured the Nd isotopes from winter (non-monsoon) collected samples from the BoB and AnS that were not filtered, while they measured Nd (and YREE) concentrations on filtered waters. It seems that the isotope composition of filtered seawater in the BoB is a function of mixing between a very low concentration radiogenic endmember we encountered after the rain event in March 2011 and a high concentration unradiogenic endmember from the G-B river (Singh et al., 2012). Samples move away from this line with reduced Nd concentrations and a third endmember could be BoB subsurface water (Figure 9). Singh et al. (2012) considered the surface water from the south to be 100% Indonesian Through Flow water with a Nd concentration of only 7 pmol/kg and a radiogenic isotope composition of -4. This endmember (but again from Amakawa et al., 2000 so unfiltered for isotopes) plots near the low concentration samples from the AnS (Figure 9) following the rain event in March 2011 when it appears that the colloidal fraction rapidly migrated to the labile particulate pool. The remaining Nd, hypothesised to be truly dissolved, may have been sourced from Indonesian Through Flow water but as it is even more radiogenic it is more likely that more local radiogenic sources like the Indo-Burmese Ranges (Damodararao et al., 2016) also contributed. It follows that the apparent mixing between Indonesian Through Flow water and G-B outflow water masses used to explain the BoB surface water composition (Singh et al., 2012) could potentially be a function of the proportion of the filtered BoB seawater in the truly dissolved and colloidal phases (Figure 9). It seems that this proportion can be rapidly changed by interaction with the large labile particulate fraction observed here and this may also be responsible for the

observed inter-annual changes in the Nd isotope composition of BoB surface water (Yu et al., 2017a). This is an extension to the idea of Elderfield et al. (1990) that the river water REE composition is controlled by the balance between truly dissolved and colloidal pools with the addition of a third pool, which is the labile particulate fraction. Future sampling campaigns should include both filtered and unfiltered samples for Nd isotope analyses as well as YREE concentrations, and ultrafiltration should be performed whenever logistically possible. Eventually we would hope to be able to carry out residence time calculations, such as performed by Amakawa et al. (2000) and revisited by Yu et al., (2017b), for the YREE in each pool individually. The labile particulate pool may also help to explain variations in seawater Nd isotopes in the entire oceanic water column on times scale of years observed in other regions (Grasse et al., 2017).

CONCLUSIONS

The dissolved YREE composition of filtered seawater around the Andaman Islands reveals both local input to and removal of YREE from the dissolved phase. Rapid removal following an exceptional rainfall event in March 2011 left the remaining Nd with a markedly radiogenic isotope composition and as a result of this, the dissolved Nd isotope composition varies by some 7 εNd units across the islands. Changes in the YREE and Nd isotope composition within one year are observed at 3 fixed locations confirming recent suggestions that short-term temporal variations occur in the BoB. The similarity of YREE patterns across the BoB and AnS suggests a common source for their enrichment in Indian Ocean surface waters. Taken together the data for surface waters from this study and the literature appear to form a mixing relationship but we hypothesise that this reflects the proportions of radiogenic Nd in the truly dissolved phase and of unradiogenic Nd in the colloidal pool. Based on comparison of filtered and unfiltered samples a third phase, a labile particulate pool, is identified which controls the proportion of dissolved YREE phases by removing the colloidal fraction. This control by particulate YREE phases is likely also important in other sediment and particle rich regions.

AUTHOR CONTRIBUTIONS

EH and PMM collected the samples. EH performed the analyses and wrote the manuscript with contributions from MF and PMM.

ACKNOWLEDMENTS

We thank the National Geographic Committee for Exploration for funding the fieldwork on the Andaman Islands and Sachin, Das and numerous fishermen for their assistance in the field. We are grateful to the Andaman & Nicobar Administration Wildlife Division for allowing water sampling and in particular the officers in Mayabunder for their assistance. Katharina Pahnke-May and Philip Böning from the ICBM at the University of Oldenburg helped with the low concentration Nd isotope measurements using their Neptune MC-ICPMS and Eric Achterberg at GEOMAR and Christian

Schlosser are thanked for use of their seaFAST and Element XR instrument, as well as for scientific discussion.

REFERENCES

Adebayo, S. B., Cui, M., Hong, T., White, C. D., Martin, E. E., and Johannesson, K. H. (2018). Rare Earth Elements Geochemistry and Nd Isotopes in the Mississippi River and Gulf of Mexico Mixing Zone. *Frontiers in Marine Science* 5. doi:10.3389/fmars.2018.00166.

Akhil, V. P., Durand, F., Lengaigne, M., Vialard, J., Keerthi, M. G., Gopalakrishna, V. V., et al. (2014). A modeling study of the processes of surface salinity seasonal cycle in the Bay of Bengal. *Journal of Geophysical Research: Oceans* 119, 3926–3947. doi:10.1002/2013JC009632.

Akhil, V. P., Lengaigne, M., Vialard, J., Durand, F., Keerthi, M. G., Chaitanya, A. V. S., et al. (2016). A modeling study of processes controlling the Bay of Bengal sea surface salinity interannual variability. *Journal of Geophysical Research: Oceans* 121, 8471–8495. doi:10.1002/2016JC011662.

Ali, S., Hathorne, E. C., Frank, M., Gebregiorgis, D., Stattegger, K., Stumpf, R., et al. (2015). South Asian monsoon history over the past 60 kyr recorded by radiogenic isotopes and clay mineral assemblages in the Andaman Sea. *Geochemistry, Geophysics, Geosystems* 16, 505–521. doi:10.1002/2014GC005586.

Alibo, D. S., and Nozaki, Y. (1999). Rare earth elements in seawater: particle association, shale-normalization, and Ce oxidation. Geochimica et Cosmochimica Acta 63, 363–372. doi:10.1016/S0016-7037(98)00279-8.

Alibo, D.S., and Nozaki, Y. (2004). Dissolved rare earth elements in the eastern Indian Ocean: chemical tracers of the water masses. *Deep Sea Research Part I: Oceanographic Research Papers* 51, 559–576. doi:10.1016/j.dsr.2003.11.004.

Allen, R., Carter, A., Najman, Y., Bandopadhyay, P. C., Chapman, H. J., Bickle, M. J., et al. (2008a). "New constraints on the sedimentation and uplift history of the Andaman-Nicobar accretionary prism, South Andaman Island," in *Special Paper 436: Formation and Applications of the Sedimentary Record in Arc Collision Zones* (Geological Society of America), 223–255. doi:10.1130/2008.2436(11).

Allen, R., Najman, Y., Carter, A., Barfod, D., Bickle, M. J., Chapman, H. J., et al. (2008b). Provenance of the Tertiary sedimentary rocks of the Indo-Burman Ranges, Burma (Myanmar): Burman arc or Himalayan-derived? *Journal of the Geological Society* 165, 1045–1057. doi:10.1144/0016-76492007-143.

Amakawa, H., Alibo, D. S., and Nozaki, Y. (2000). Nd isotopic composition and REE pattern in the surface waters of the eastern Indian Ocean and its adjacent seas. *Geochimica et Cosmochimica Acta* 64, 1715–1727. doi:10.1016/S0016-7037(00)00333-1.

Bau, M. (1996). Controls on the fractionation of isovalent trace elements in magmatic and aqueous systems: evidence from Y/Ho, Zr/Hf, and lanthanide tetrad effect. *Contributions to Mineralogy and Petrology* 123, 323–333. doi:10.1007/s004100050159.

Bau, M. (1999). Scavenging of dissolved yttrium and rare earths by precipitating iron oxyhydroxide: experimental evidence for Ce oxidation, Y-Ho fractionation, and lanthanide tetrad effect. *Geochimica et Cosmochimica Acta* 63, 67–77. doi:10.1016/S0016-7037(99)00014-9.

Bertram, C. J., and Elderfield, H. (1993). The geochemical balance of the rare earth elements and neodymium isotopes in the oceans. *Geochimica et Cosmochimica Acta* 57, 1957–1986. doi:10.1016/0016-7037(93)90087-D.
Byrne, R. H., Lee, J. H., and Bingler, L. S. (1991). Rare earth element complexation by PO43− ions in aqueous solution. Geochimica et Cosmochimica Acta 55, 2729–2735. doi:10.1016/0016-7037(91)90439-C.
Cantrell, K. J., and Byrne, R. H. (1987). Rare earth element complexation by carbonate and oxalate ions. *Geochimica et Cosmochimica Acta* 51, 597–605. doi:10.1016/0016-7037(87)90072-X.
Chaitanya, A. V. S., Durand, F., Mathew, S., Gopalakrishna, V. V., Papa, F., Lengaigne, M., et al. (2015). Observed year-to-year sea surface salinity variability in the Bay of Bengal during the 2009–2014 period. *Ocean Dynamics* 65, 173–186. doi:10.1007/s10236-014-0802-x.
Chatterjee, A., Shankar, D., McCreary, J. P., Vinayachandran, P. N., and Mukherjee, A. (2017). Dynamics of Andaman Sea circulation and its role in connecting the equatorial Indian Ocean to the Bay of Bengal. *Journal of Geophysical Research: Oceans* 122, 3200–3218. doi:10.1002/2016JC012300.
Chatterjee, A., Shankar, D., Shenoi, S. S. C., Reddy, G. V., Michael, G. S., Ravichandran, M., et al. (2012). A new atlas of temperature and salinity for the North Indian Ocean. *Journal of Earth System Science* 121, 559–593. doi:10.1007/s12040-012-0191-9.
Colin, C., Turpin, L., Bertaux, J., Desprairies, A., and Kissel, C. (1999). Erosional history of the Himalayan and Burman ranges during the last two glacial–interglacial cycles. *Earth and Planetary Science Letters* 171, 647–660. doi:10.1016/S0012-821X(99)00184-3.
Curray, J. R., Emmel, F. J., and Moore, D. G. (2002). The Bengal Fan: morphology, geometry, stratigraphy, history and processes. *Marine and Petroleum Geology* 19, 1191–1223. doi:10.1016/S0264-8172(03)00035-7.
Dai, A., Qian, T., Trenberth, K. E., and Milliman, J. D. (2009). Changes in Continental Freshwater Discharge from 1948 to 2004. *Journal of Climate* 22, 2773–2792. doi:10.1175/2008JCLI2592.1.
Damodararao, K., Singh, S. K., Rai, V. K., Ramaswamy, V., and Rao, P. S. (2016). Lithology, Monsoon and Sea-Surface Current Control on Provenance, Dispersal and Deposition of Sediments over the Andaman Continental Shelf. *Frontiers in Marine Science* 3. doi:10.3389/fmars.2016.00118.
Duncombe, J. Making Sense of Landslide Danger After Kerala's Floods - Eos. *Eos* 99, 7.
Durand, F., Papa, F., Rahman, A., and Bala, S. K. (2011). Impact of Ganges–Brahmaputra interannual discharge variations on Bay of Bengal salinity and temperature during 1992–1999 period. *Journal of Earth System Science* 120, 859–872. doi:10.1007/s12040-011-0118-x.
Elderfield, H. (1988). The oceanic chemistry of the rare-earth elements. *Philos Trans R Soc Lond A* 325, 105. doi:10.1098/rsta.1988.0046.
Elderfield, H., Upstill-Goddard, R., and Sholkovitz, E. R. (1990). The rare earth elements in rivers, estuaries, and coastal seas and their significance to the composition of

ocean waters. *Geochimica et Cosmochimica Acta* 54, 971–991. doi: 10.1016/0016-7037(90)90432-K.
Fasullo, J., and Webster, P. J. (2003). A Hydrological Definition of Indian Monsoon Onset and Withdrawal. *J. Climate* 16, 3200–3211. doi:10.1175/1520-0442(2003)016
Frank, M. (2002). Radiogenic isotopes: Tracers of past ocean circulation and erosional input. *Reviews of Geophysics* 40. doi:10.1029/2000RG000094.
Freslon, N., Bayon, G., Toucanne, S., Bermell, S., Bollinger, C., Chéron, S., et al. (2014). Rare earth elements and neodymium isotopes in sedimentary organic matter. *Geochimica et Cosmochimica Acta* 140, 177–198. doi:10.1016/j.gca.2014.05.016
Gadgil, S., and Gadgil, S. (2006) The Indian Monsoon, GDP and agriculture. Economic and political weekly, 4887. doi: 10.2307/4418949
Garzanti, E., Limonta, M., Resentini, A., Bandopadhyay, P. C., Najman, Y., Andò, S., et al. (2013). Sediment recycling at convergent plate margins (Indo-Burman Ranges and Andaman–Nicobar Ridge). *Earth-Science Reviews* 123, 113–132. doi:10.1016/j.earscirev.2013.04.008.
Giosan, L., Naing, T., Min Tun, M., Clift, P. D., Filip, F., Constantinescu, S., et al. (2018). On the Holocene evolution of the Ayeyawady megadelta. *Earth Surf. Dynam.* 6, 451–466. doi:10.5194/esurf-6-451-2018.
Girishkumar, M. S., Ravichandran, M., McPhaden, M. J., and Rao, R. R. (2011). Intraseasonal variability in barrier layer thickness in the south central Bay of Bengal. *Journal of Geophysical Research* 116. doi:10.1029/2010JC006657.
Girishkumar, M. S., M. Ravichandran, and M. J. McPhaden (2013), Temperature inversions and their influence on the mixed layer heat budget during the winters of 2006–2007 and 2007–2008 in the Bay of Bengal, *J. Geophys. Res. Oceans*, 118, 3336–3349, doi:10.1002/jgrc.20192.
Goldstein, S. J., and Jacobsen, S. B. (1987) The Nd and Sr isotopic systematics of river-water dissolved material: implications for the sources of Nd and Sr in seawater. Chemical Geology, 66, 245-272. doi.org/10.1016/0168-9622(87)90045-5
Goldstein, S. J., and Jacobsen, S. B. (1988a). Rare earth elements in river waters. *Earth and Planetary Science Letters* 89, 35–47. doi:10.1016/0012-821X(88)90031-3.
Goldstein, S. J., and Jacobsen, S. B. (1988b). Nd and Sr isotopic systematics of river water suspended material: implications for crustal evolution. *Earth and Planetary Science Letters* 87, 249–265. doi:10.1016/0012-821X(88)90013-1.
Grasse, P., Bosse, L., Hathorne, E. C., Böning, P., Pahnke, K., and Frank, M. (2017). Short-term variability of dissolved rare earth elements and neodymium isotopes in the entire water column of the Panama Basin. *Earth and Planetary Science Letters* 475, 242–253. doi:10.1016/j.epsl.2017.07.022.
Hannigan, R. E., and Sholkovitz, E. R. (2001). The development of middle rare earth element enrichments in freshwaters: weathering of phosphate minerals. *Chemical Geology* 175, 495–508. doi:10.1016/S0009-2541(00)00355-7.
Hathorne, E. C., Haley, B., Stichel, T., Grasse, P., Zieringer, M., and Frank, M. (2012). Online preconcentration ICP-MS analysis of rare earth elements in seawater. *Geochemistry, Geophysics, Geosystems* 13, doi:10.1029/2011GC003907.
Hathorne, E. C., Stichel, T., Brück, B., and Frank, M. (2015). Rare earth element distribution in the Atlantic sector of the Southern Ocean: The balance between particle

scavenging and vertical supply. Marine Chemistry 177, 157–171. doi:10.1016/j.-marchem.2015.03.011.
Hoyle, J., Elderfield, H., Gledhill, A., and Greaves, M. (1984). The behaviour of the rare earth elements during mixing of river and sea waters. *Geochimica et Cosmochimica Acta* 48, 143–149. doi:10.1016/0016-7037(84)90356-9.
Jian, J., Webster, P. J., and Hoyos, C. D. (2009). Large-scale controls on Ganges and Brahmaputra river discharge on intraseasonal and seasonal time-scales. *Quarterly Journal of the Royal Meteorological Society* 135, 353–370. doi:10.1002/qj.384.
Jochum, K. P., Nohl, U., Herwig, K., Lammel, E., Stoll, B., and Hofmann, A. W. (2005). GeoReM: A New Geochemical Database for Reference Materials and Isotopic Standards. *Geostand Geoanalyt Res* 29, 333–338. doi:10.1111/j.1751-908X.2005.tb00904.x
Kiran Kumar, P., Singh, A., and Ramesh, R. (2018). Controls on δ18O, δD and δ18O-salinity relationship in the northern Indian Ocean. Marine Chemistry 207, 55–62. doi:10.1016/j.marchem.2018.10.010.
Kraft, S., Frank, M., Hathorne, E. C., and Weldeab, S. (2013). Assessment of seawater Nd isotope signatures extracted from foraminiferal shells and authigenic phases of Gulf of Guinea sediments. *Geochimica et Cosmochimica Acta* 121, 414–435. doi:10.1016/j.gca.2013.07.029.
Krishna Kumar, K., Rupa Kumar, K., Ashrit, R. G., Deshpande, N. R., and Hansen, J. W. (2004). Climate impacts on Indian agriculture. *International Journal of Climatology* 24, 1375–1393. doi:10.1002/joc.1081.
Kurian, S., Nath, B. N., Ramaswamy, V., Naman, D., Gnaneshwar Rao, T., Kamesh Raju, K. A., et al. (2008). Possible detrital, diagenetic and hydrothermal sources for Holocene sediments of the Andaman backarc basin. *Marine Geology* 247, 178–193. doi:10.1016/j.margeo.2007.09.006.
Lacan, F., Tachikawa, K., and Jeandel, C. (2012). Neodymium isotopic composition of the oceans: A compilation of seawater data. *Chemical Geology* 300–301, 177–184. doi:10.1016/j.chemgeo.2012.01.019.
Laukert, G., Frank, M., Bauch, D., Hathorne, E. C., Rabe, B., von Appen, W.-J., et al. (2017). Ocean circulation and freshwater pathways in the Arctic Mediterranean based on a combined Nd isotope, REE and oxygen isotope section across Fram Strait. *Geochimica et Cosmochimica Acta* 202, 285–309. doi:10.1016/j.gca.2016.12.028.
Liu, Y., Lo, L., Shi, Z., Wei, K.-Y., Chou, C.-J., Chen, Y.-C., et al. (2015). Obliquity pacing of the western Pacific Intertropical Convergence Zone over the past 282,000 years. *Nat Commun* 6, 10018. doi:10.1038/ncomms10018.
Mahowald, N. M., Baker, A. R., Bergametti, G., Brooks, N., Duce, R. A., Jickells, T. D., et al. (2005). Atmospheric global dust cycle and iron inputs to the ocean. *Global Biogeochem. Cycles* 19, doi:10.1029/2004GB002402.
McNeill, L. C., Dugan, B., Backman, J., Pickering, K. T., Pouderoux, H. F. A., Henstock, T. J., et al. (2017). Understanding Himalayan erosion and the significance of the Nicobar Fan. *Earth and Planetary Science Letters* 475, 134–142. doi:10.1016/j.epsl.2017.07.019.
Merschel, G., Bau, M., and Dantas, E. L. (2017a). Contrasting impact of organic and inorganic nanoparticles and colloids on the behavior of particle-reactive elements in

tropical estuaries: An experimental study. *Geochimica et Cosmochimica Acta* 197, 1–13. doi:10.1016/j.gca.2016.09.041.
Merschel, G., Bau, M., Schmidt, K., Münker, C., and Dantas, E. L. (2017b). Hafnium and neodymium isotopes and REY distribution in the truly dissolved, nanoparticulate/colloidal and suspended loads of rivers in the Amazon Basin, Brazil. *Geochimica et Cosmochimica Acta* 213, 383–399. doi:10.1016/j.gca.2017.07.006.
Milliman, J. D., and Syvitski, J. P. M. (1992). Geomorphic/Tectonic Control of Sediment Discharge to the Ocean: The Importance of Small Mountainous Rivers. *The Journal of Geology* 100, 525–544. doi:10.1086/629606.
Moffett, J. W. (1994). The relationship between cerium and manganese oxidation in the marine environment. *Limnology and Oceanography* 39, 1309–1318. doi:10.4319/lo.1994.39.6.1309.
Nance, W., and Taylor, S. . (1976). Rare earth element patterns and crustal evolution—I. Australian post-Archean sedimentary rocks. *Geochimica et Cosmochimica Acta* 40, 1539–1551. doi:10.1016/0016-7037(76)90093-4.
Nilsson-Kerr, K., Anand, P., Sexton, P. F., Leng, M. J., Misra, S., Clemens, S. C., et al. (2019). Role of Asian summer monsoon subsystems in the inter-hemispheric progression of deglaciation. *Nat. Geosci.* doi:10.1038/s41561-019-0319-5.
Nozaki, Y., and Alibo, D. S. (2003) Importance of vertical geochemical processes in controlling the oceanic profiles of dissolved rare earth elements in the northeastern Indian Ocean. *Earth and Planetary Science Letters*, 205, 155–172.
Nozaki, Y., Zhang, J., and Amakawa, H. (1997). The fractionation between Y and Ho in the marine environment. *Earth and Planetary Science Letters* 148, 329–340. doi:10.1016/S0012-821X(97)00034-4.
Osborne, A. H., Haley, B. A., Hathorne, E. C., Plancherel, Y., and Frank, M. (2015). Rare earth element distribution in Caribbean seawater: Continental inputs versus lateral transport of distinct REE compositions in subsurface water masses. *Marine Chemistry* 177, 172–183. doi:10.1016/j.marchem.2015.03.013.
Osborne, A. H., Hathorne, E. C., Schijf, J., Plancherel, Y., Böning, P., and Frank, M. (2017). The potential of sedimentary foraminiferal rare earth element patterns to trace water masses in the past. *Geochemistry, Geophysics, Geosystems* 18, 1550–1568. doi:10.1002/2016GC006782.
Pal, T., Gupta, T. D., Chakraborty, P. P., and Gupta, S. C. D. (2005). Pyroclastic deposits of Mio-Pliocene age in the Arakan Yoma-Andaman-Java subduction complex, Andaman Islands, Bay of Bengal, India. *Geochemical Journal* 39, 69–82. doi:10.2343/geochemj.39.69.
Pant, V., Girishkumar, M. S., Udaya Bhaskar, T. V. S., Ravichandran, M., Papa, F., and Thangaprakash, V. P. (2015). Observed interannual variability of near-surface salinity in the Bay of Bengal: Salinity variability in the BoB. *Journal of Geophysical Research: Oceans* 120, 3315–3329. doi:10.1002/2014JC010340.
Quinn, K. A., Byrne, R. H., and Schijf, J. (2006). Sorption of yttrium and rare earth elements by amorphous ferric hydroxide: Influence of solution complexation with carbonate. *Geochimica et Cosmochimica Acta* 70, 4151–4165. doi:10.1016/j.gca.2006.06.014.
Ramaswamy, V., Rao, P. ., Rao, K. ., Thwin, S., Rao, N. S., and Raiker, V. (2004). Tidal influence on suspended sediment distribution and dispersal in the northern An-

daman Sea and Gulf of Martaban. *Marine Geology* 208, 33–42. doi:10.1016/j.margeo.2004.04.019.
Rengarajan, R., and Sarin, M. M. (2004). Distribution of rare earth elements in the Yamuna and the Chambal rivers, India. *Geochemical Journal* 38, 551–569. doi:10.2343/geochemj.38.551.
Rizal, S., Damm, P., Wahid, M.A., Sundermann, J., Ilhamsyah, Y., Iskandar T., and Muhammad (2012). General circulation in the Malacca Strait and Andaman Sea: a numerical model study. *American Journal of Environmental Sciences* 8, 479–488. doi:10.3844/ajessp.2012.479.488.
Roberts, N. L., Piotrowski, A. M., McManus, J. F., and Keigwin, L. D. (2010). Synchronous Deglacial Overturning and Water Mass Source Changes. *Science* 327, 75–78. doi:10.1126/science.1178068.
Roberts, N. L., Piotrowski, A. M., Elderfield, H., Eglinton, T. I., and Lomas, M. W. (2012). Rare earth element association with foraminifera. *Geochimica et Cosmochimica Acta* 94, 57–71. doi:10.1016/j.gca.2012.07.009.
Rousseau, T. C. C., Sonke, J. E., Chmeleff, J., van Beek, P., Souhaut, M., Boaventura, G., et al. (2015). Rapid neodymium release to marine waters from lithogenic sediments in the Amazon estuary. *Nature Communications* 6. doi:10.1038/ncomms8592.
Saha, N., Webb, G. E., and Zhao, J.-X. (2016). Coral skeletal geochemistry as a monitor of inshore water quality. *Science of The Total Environment* 566–567, 652–684. doi:10.1016/j.scitotenv.2016.05.066.
Sarkar, S., and Ghosh, A. K. (2013). Coral bleaching a nemesis for the Andaman reefs: Building an improved conservation paradigm. *Ocean & Coastal Management* 71, 153–162. doi:10.1016/j.ocecoaman.2012.09.010.
Sarkar, S., and Ghosh, A. K. (2015). Evaluation of coralline algal diversity from the Serravallian carbonate sediments of Little Andaman Island (Hut Bay), India. *Carbonates and Evaporites* 30, 13–24. doi:10.1007/s13146-014-0190-9.
Schlosser, C., Schmidt, K., Aquilina, A., Homoky, W. B., Castrillejo, M., Mills, R. A., et al. (2018). Mechanisms of dissolved and labile particulate iron supply to shelf waters and phytoplankton blooms off South Georgia, Southern Ocean. *Biogeosciences* 15, 4973–4993. doi:10.5194/bg-15-4973-2018.
Sengupta, D., Bharath Raj, G. N., Ravichandran, M., Sree Lekha, J., and Papa, F. (2016). Near-surface salinity and stratification in the north Bay of Bengal from moored observations: Salinity in the North Bay of Bengal. *Geophysical Research Letters* 43, 4448–4456. doi:10.1002/2016GL068339.
Sengupta, D., Bharath Raj, G. N., and Shenoi, S. S. C. (2006). Surface freshwater from Bay of Bengal runoff and Indonesian Throughflow in the tropical Indian Ocean. *Geophysical Research Letters* 33. doi:10.1029/2006GL027573.
Shaman, J., Cane, M., and Kaplan, A. (2005). The relationship between Tibetan snow depth, ENSO, river discharge and the monsoons of Bangladesh. *International Journal of Remote Sensing* 26, 3735–3748. doi:10.1080/01431160500185599.
Shiller, A. M. (2002). Seasonality of dissolved rare earth elements in the lower Mississippi River. *Geochemistry, Geophysics, Geosystems* 3, 1–14. doi:10.1029/2002GC000372.
Sholkovitz, E. R. (1995). The aquatic chemistry of rare earth elements in rivers and estuaries. *Aquatic Geochemistry* 1, 1–34. doi:10.1007/BF01025229.

Sholkovitz, E. R., Church, T. M., and Arimoto, R. (1993). Rare Earth element composition of precipitation, precipitation particles, and aerosols. *Journal of Geophysical Research* 98, 20587. doi:10.1029/93JD01926.
Sholkovitz, E. R., and Elderfield, H. (1988). Cycling of dissolved rare earth elements in Chesapeake Bay. *Global Biogeochemical Cycles* 2, 157–176. doi:10.1029/GB002i002p00157.
Sholkovitz, E. R., Landing, W. M., and Lewis, B. L. (1994). Ocean particle chemistry: The fractionation of rare earth elements between suspended particles and seawater. *Geochimica et Cosmochimica Acta* 58, 1567–1579. doi:10.1016/0016-7037(94)90559-2.
Sholkovitz, E., and Szymczak, R. (2000). The estuarine chemistry of rare earth elements: comparison of the Amazon, Fly, Sepik and the Gulf of Papua systems. *Earth and Planetary Science Letters* 179, 299–309. doi:10.1016/S0012-821X(00)00112-6.
Singh, S. K., and France-Lanord, C. (2002). Tracing the distribution of erosion in the Brahmaputra watershed from isotopic compositions of stream sediments. *Earth and Planetary Science Letters* 202, 645–662. doi:10.1016/S0012-821X(02)00822-1.
Singh, S. P., Singh, S. K., Goswami, V., Bhushan, R., and Rai, V. K. (2012). Spatial distribution of dissolved neodymium and εNd in the Bay of Bengal: Role of particulate matter and mixing of water masses. *Geochimica et Cosmochimica Acta* 94, 38–56. doi:10.1016/j.gca.2012.07.017.
Skinner, L. C., Sadekov, A., Brandon, M., Greaves, M., Plancherel, Y., de la Fuente, M., et al. (2019). Rare Earth Elements in early-diagenetic foraminifer 'coatings': Pore-water controls and potential palaeoceanographic applications. *Geochimica et Cosmochimica Acta* 245, 118–132. doi:10.1016/j.gca.2018.10.027.
Srinivas, B., and Sarin, M. M. (2013). Atmospheric dry-deposition of mineral dust and anthropogenic trace metals to the Bay of Bengal. *Journal of Marine Systems* 126, 56–68. doi:10.1016/j.jmarsys.2012.11.004.
Stichel, T., Frank, M., Rickli, J., and Haley, B. A. (2012). The hafnium and neodymium isotope composition of seawater in the Atlantic sector of the Southern Ocean. *Earth and Planetary Science Letters* 317–318, 282–294. doi:10.1016/j.epsl.2011.11.025.
Tachikawa, K., Jeandel, C., and Roy-Barman, M. (1999). A new approach to the Nd residence time in the ocean: the role of atmospheric inputs. *Earth and Planetary Science Letters* 170, 433–446. doi:10.1016/S0012-821X(99)00127-2.
Tachikawa, K., Toyofuku, T., Basile-Doelsch, I., and Delhaye, T. (2013). Microscale neodymium distribution in sedimentary planktonic foraminiferal tests and associated mineral phases. *Geochimica et Cosmochimica Acta* 100, 11–23. doi:10.1016/j.gca.2012.10.010.
Tanaka, T., Togashi, S., Kamioka, H., Amakawa, H., Kagami, H., Hamamoto, T., et al. (2000). JNdi-1: a neodymium isotopic reference in consistency with LaJolla neodymium. *Chemical Geology* 168, 279–281. doi:10.1016/S0009-2541(00)00198-4.
Tang, J., and Johannesson, K. H. (2010). Ligand extraction of rare earth elements from aquifer sediments: Implications for rare earth element complexation with organic matter in natural waters. *Geochimica et Cosmochimica Acta* 74, 6690–6705. doi:10.1016/j.gca.2010.08.028.

Thadathil, P., Muraleedharan, P. M., Rao, R. R., Somayajulu, Y. K., Reddy, G. V., and Revichandran, C. (2007). Observed seasonal variability of barrier layer in the Bay of Bengal. *Journal of Geophysical Research* 112. doi:10.1029/2006JC003651.
Turner, A. G., and Annamalai, H. (2012). Climate change and the South Asian summer monsoon. *Nature Climate Change* 2, 587–595. doi:10.1038/nclimate1495.
Unger, D., Ittekkot, V., Schäfer, P., Tiemann, J., and Reschke, S. (2003). Seasonality and interannual variability of particle fluxes to the deep Bay of Bengal: influence of riverine input and oceanographic processes. *Deep Sea Research Part II: Topical Studies in Oceanography* 50, 897–923. doi:10.1016/S0967-0645(02)00612-4.
van de Flierdt, T., Griffiths, A. M., Lambelet, M., Little, S. H., Stichel, T., and Wilson, D. J. (2016). Neodymium in the oceans: a global database, a regional comparison and implications for palaeoceanographic research. *Philosophical Transactions of the Royal Society A: Mathematical, Physical and Engineering Sciences* 374, 20150293. doi: 10.1098/rsta.2015.0293.
van de Flierdt, T., Pahnke, K., Amakawa, H., Andersson, P., Basak, C., Coles, B., et al. (2012). GEOTRACES intercalibration of neodymium isotopes and rare earth element concentrations in seawater and suspended particles. Part 1: reproducibility of results for the international intercomparison: Intercalibration of Seawater Nd Isotopes. *Limnology and Oceanography: Methods* 10, 234–251. doi:10.4319/lom.2012.10.234.
van Geldern, R., and Barth, J. A. C. (2012). Optimization of instrument setup and post-run corrections for oxygen and hydrogen stable isotope measurements of water by isotope ratio infrared spectroscopy (IRIS): Water stable isotope analysis with IRIS. *Limnology and Oceanography: Methods* 10, 1024–1036. doi:10.4319/lom. 2012.10.1024.
Varkey, M. J., V. S. N. Murty, and A. Suryanarayana (1996), Physical oceanography of the Bay of Bengal and Andaman Sea, Oceanogr. Mar. Biol., 34, 1–70.
Wyndham, T., McCulloch, M., Fallon, S., and Alibert, C. (2004). High-resolution coral records of rare earth elements in coastal seawater: biogeochemical cycling and a new environmental proxy. *Geochimica et Cosmochimica Acta* 68, 2067–2080. doi: 10.1016/j.gca.2003.11.004.
Yu, Z., Colin, C., Douville, E., Meynadier, L., Duchamp-Alphonse, S., Sepulcre, S., et al. (2017a). Yttrium and rare earth element partitioning in seawaters from the Bay of Bengal. *Geochemistry, Geophysics, Geosystems* 18, 1388–1403. doi: 10.1002/2016GC006749.
Yu, Z., Colin, C., Meynadier, L., Douville, E., Dapoigny, A., Reverdin, G., et al. (2017b). Seasonal variations in dissolved neodymium isotope composition in the Bay of Bengal. *Earth and Planetary Science Letters* 479, 310–321. doi:10.1016/j.epsl. 2017.09.022.

FIGURE CAPTIONS

Figure 1. Regional Map of the Bay of Bengal and Andaman Sea showing the mouths of the big four rivers; Ganga and Brahmaputra (G-B), Irrawaddy or Ayeyawady (I) and Salween (S), the Andaman Islands and the WOA2013 sea surface salinity clima-

tology for November (1955-2012). This figure was made using Ocean Data View (Schlitzer, R., Ocean Data View, http://odv.awi.de, 2016). Other features of interest are marked; Indo-Burmese Ranges (IBR), Gulf of Martaban (GoM) and the two deep channels connecting the Bay of Bengal (BoB) and the Andaman Sea (AnS). The sampling stations from the other studies of seawater Nd isotopes and REE in the region are shown; Labeled circles for Amakawa et al. (2000), square rhombuses for Singh et al., (2012) and triangles for Yu et al. (2017ab).

Figure 2. Maps of sample salinity during sampling in a) March 2011, b) November 2011, and c) March 2013. The locations of islands mentioned throughout the text are shown. N = North Andaman, M = Middle Andaman, S = South Andaman, JB = Jolly Buoy. This figure was made using Ocean Data View (Schlitzer, R., Ocean Data View, http://odv.awi.de, 2016).

Figure 3. Andaman Island district monthly rainfall before and during sampling (data from INDIA METEOROLOGICAL DEPARTMENT Hydromet division reports).

Figure 4. Filtered seawater samples shale normalised to PAAS (Nance and Taylor, 1976). Samples from the main locations use the same symbols: squares for Smith Is., vertical triangles for Avis Is., square rhombuses for Niel (Shaheed Dweep) Is., and horizontal triangles for Little Andaman Is.

Figure 5. Shale (PAAS; Nance and Taylor, 1976) normalised REE patterns for freshwater samples including the Ganges tributary Yamuna from Rengarajan and Sarin (2004) and the average of the 3 rain samples. The two panels are the same data but plotted on log and linear scales. For the rain samples Tm and Lu were below detection limits.

Figure 6. Shale (PAAS; Nance and Taylor, 1976) normalised REE patterns for Smith and Avis island time series. The Nd isotope composition measured for samples from March and November are marked with the same colour as the associated REE pattern.

Figure 7. Jolly Buoy Island YREE time series shale (PAAS; Nance and Taylor, 1976) and Andaman Sea Surface water (ASSW) normalised (PA10 <0.04 micron dissolved phase from Nozaki and Alibo, 2003).

Figure 8. Jolly Buoy Island time series of Nd isotope composition and Nd concentration with measured salinity

Figure 9. Radiogenic Nd isotope composition vs Nd concentration for all large volume samples of this study together with values from the literature (Amakawa et al., 2000; Singh et al., 2012; Yu et al., 2017a, b) for samples from the upper 50m water depth of the BoB and AnS (Figure 1). Together, these data (excluding sample AN12) give a correlation coefficient value of $r^2 = 0.75$. AN12 is plotted as the "Inshore Andaman Input" sample. Sediment Nd isotope values from potential sources are shown along the y-axis for the Ayeyawady (Irrawaddy) (Allen et al.,2008a; Giosan et al., 2018 , for the Andaman Islands (Ali et al., 2015), and for the Ganga-Brahmaputra

(Singh and France-Lanord, 2002, and references therein). Note the one Irrawaddy value from Colin et al. (1999) which has no location information is less radiogenic than the other Ayeyawady samples and is more similar to the Yangon or Sittaung rivers located nearby (Giosan et al., 2018). The mixing line between Indonesian through flow waters (IW) with Ganga-Brahmaputra low salinity surface water (GB) employs the end members from Singh et al. (2012) and Amakawa et al. (2000). This cannot account for the lowest concentrations and most radiogenic samples (note that the IW endmember was not filtered for isotope analysis) and much of the data from the literature fall off the mixing line due to lower Nd concentrations.

Figure 10. Selected samples normalised to North Pacific Deep water (NPDW) after Alibo and Nozaki (1999). The two surface samples measured by Amakawa et al. (2000) in the BoB and AnS and Circumpolar Deep Water (CDW) from the Southern Ocean taken from Hathorne et al. (2015) are plotted for comparison.

Figure 11. Left hand panel; Low REE concentration samples compared to <1 kDa truly dissolved fraction from the Amazon tributary Solimões (Merschel et al., 2017b). Right hand panel; Selected samples normalised to Andaman Sea Surface Water ASSW) normalised (PA10 <0.04 micron dissolved phase from Nozaki and Alibo, 2003).

Figure 12. Left hand panel; Unfiltered seawater samples and BHVO-2 basalt values (taken from GeoReM database Jochum et al., 2005) normalised to PAAS (Nance and Taylor, 1976). Right hand panel; Unfiltered YREE/filtered YREE for various examples. Samples from the main locations use the same symbols: squares for Smith Is., vertical triangles for Avis Is., square rhombuses for Niel (Shaheed Dweep) Is., and horizontal triangles for Little Andaman Is.

Figure 13. Radiogenic Nd isotope composition vs YREE indices for samples of this study together with values from the literature (Amakawa et al., 2000; Yu et al., 2017a, b) for samples from the upper 50m water depth of the BoB and AnS (Figure 1).

Figure 1.JPEG

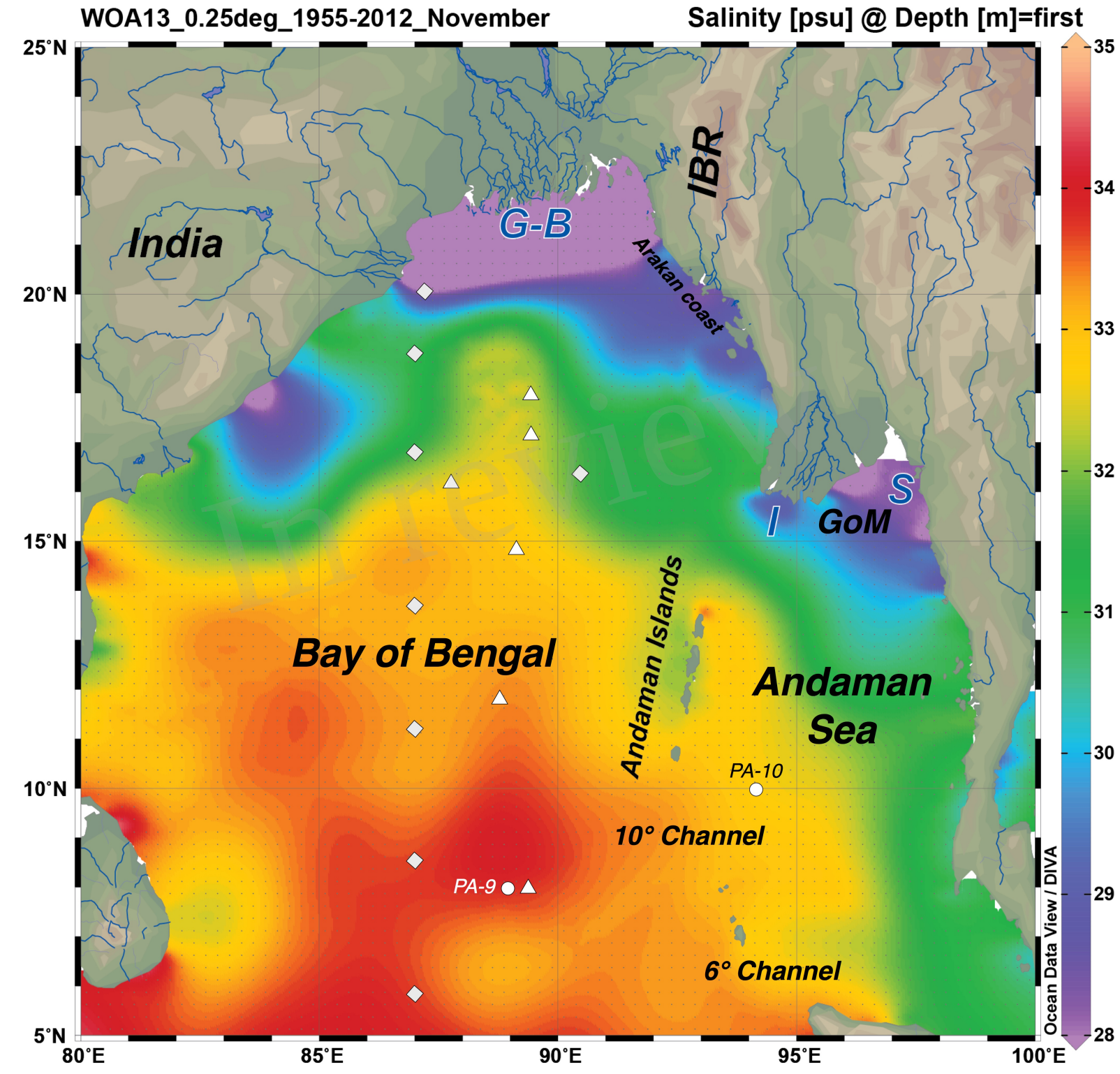

Figure 2.JPEG

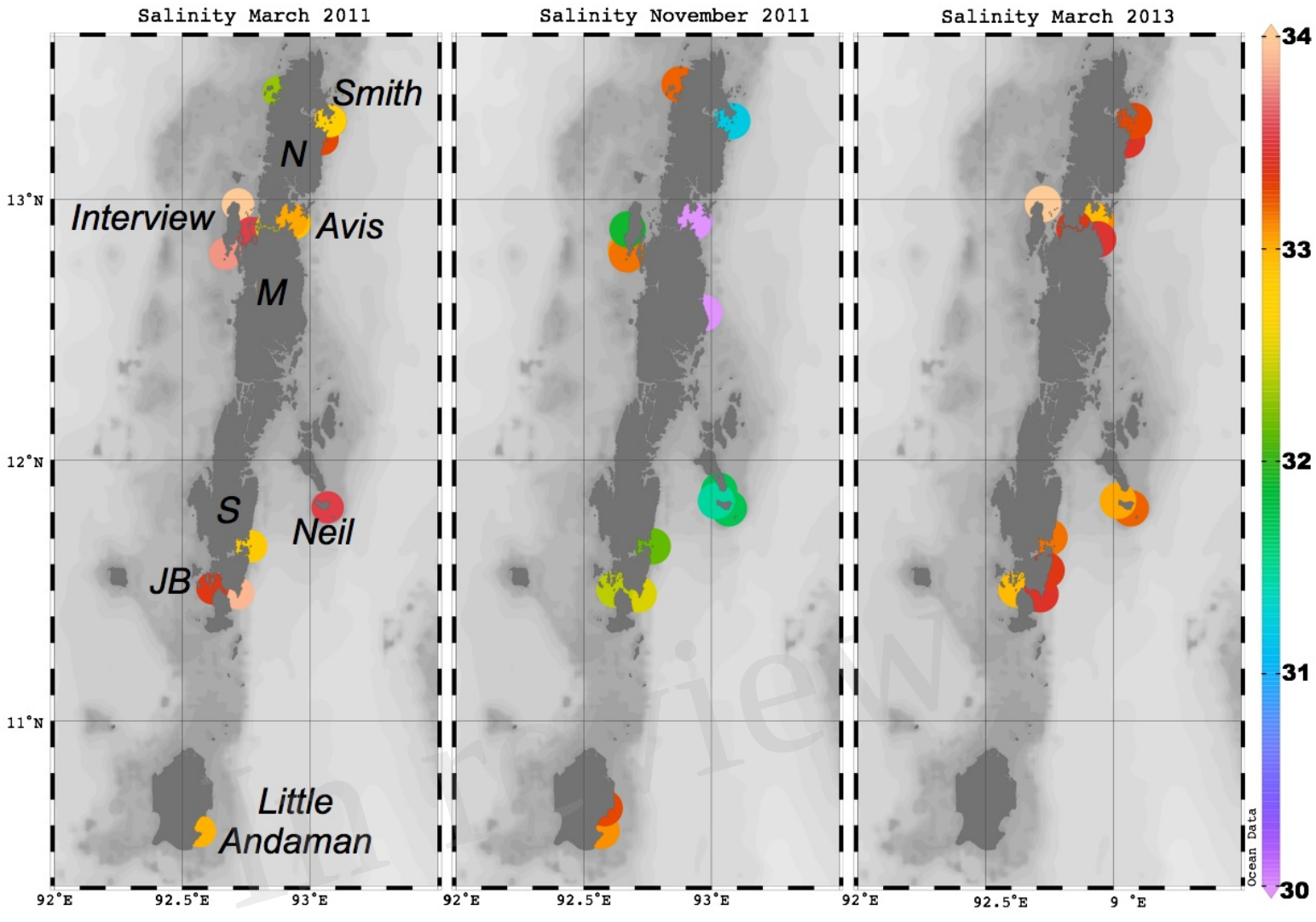

Figure 3.JPEG

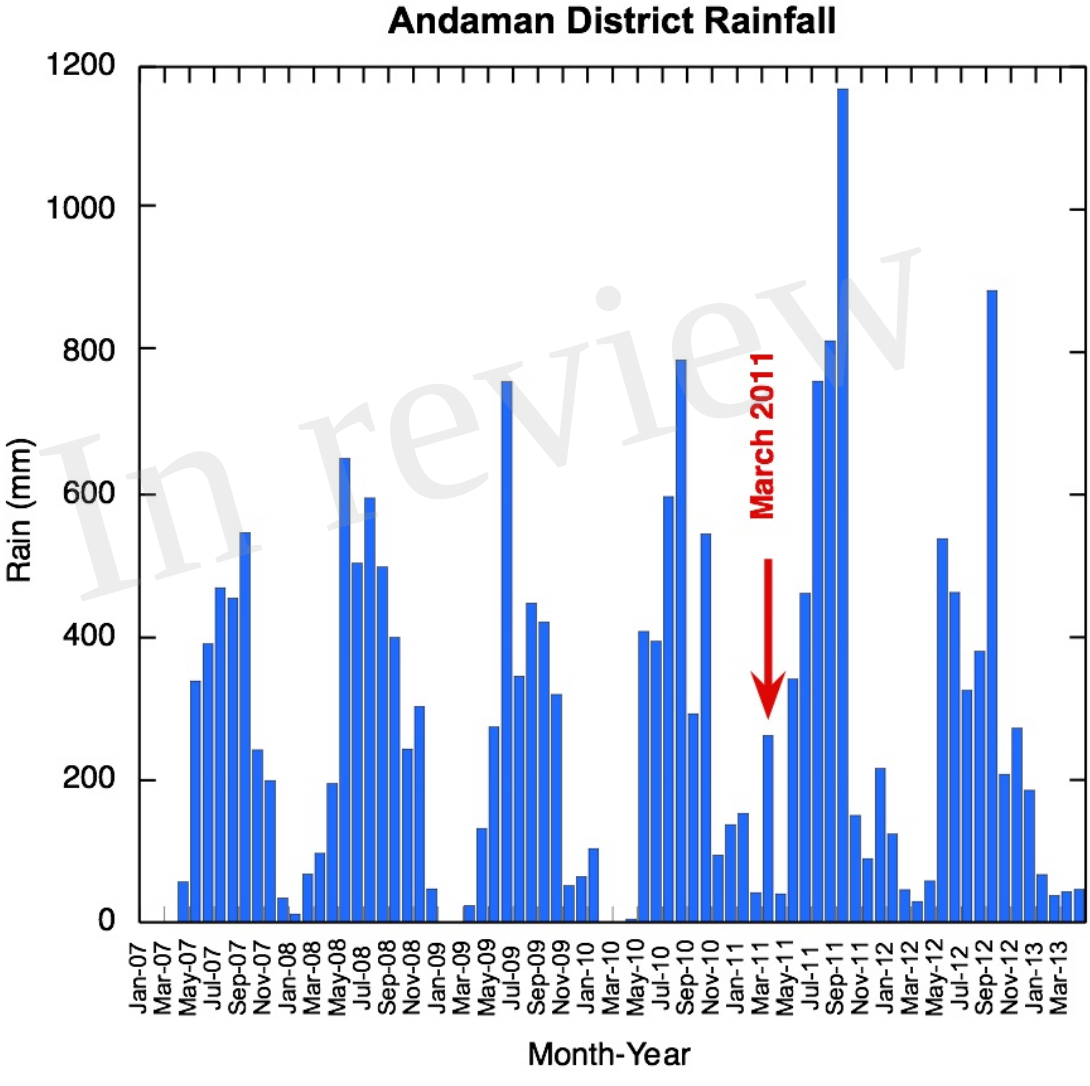

Figure 4.JPEG

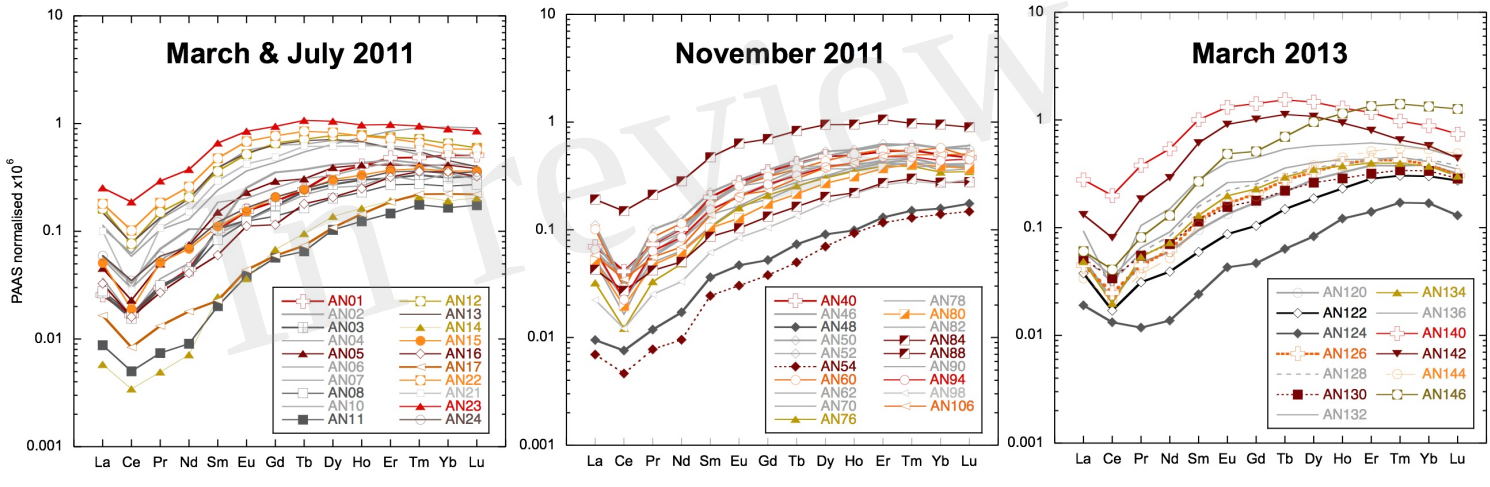

Figure 5.JPEG

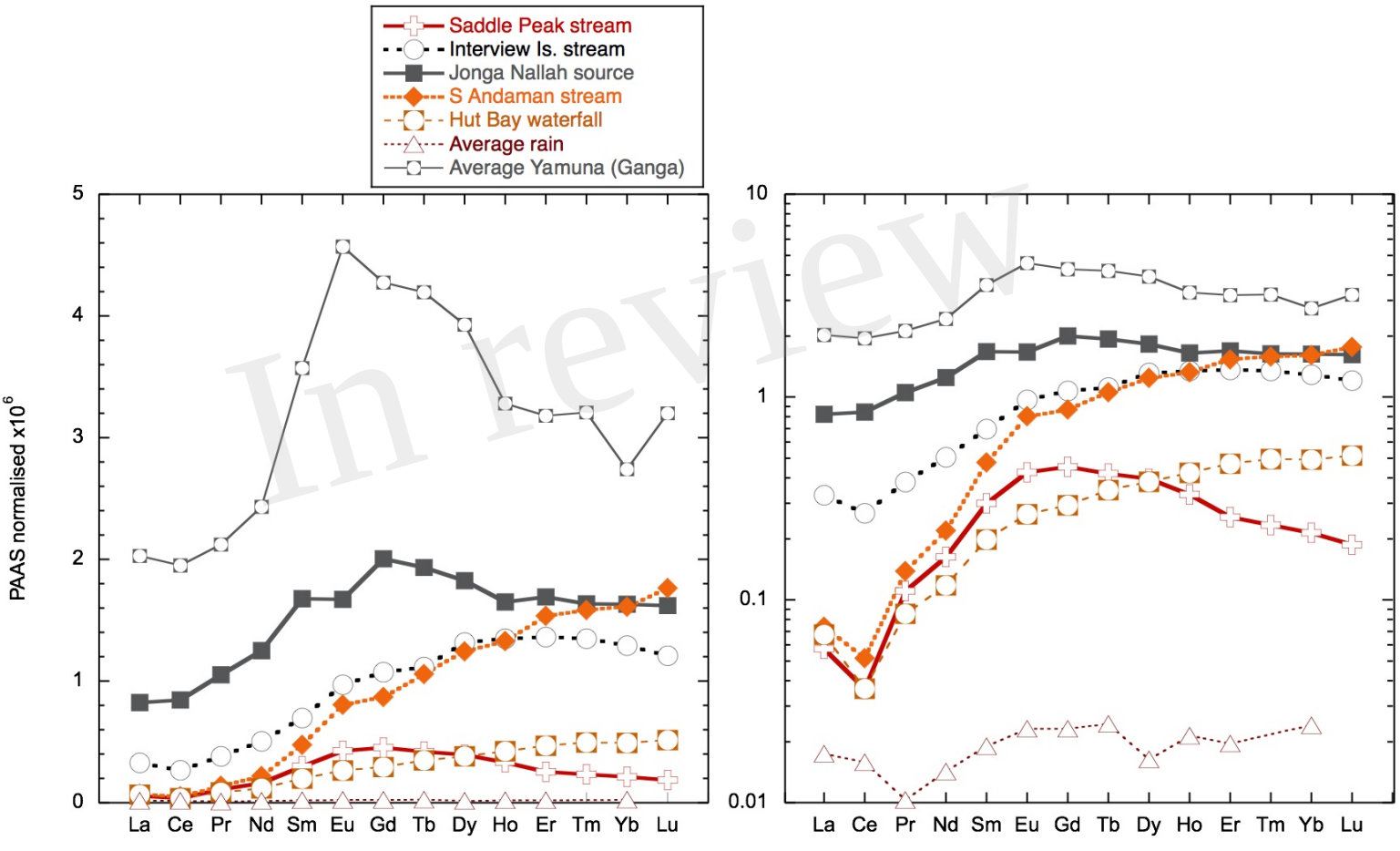

Figure 6.JPEG

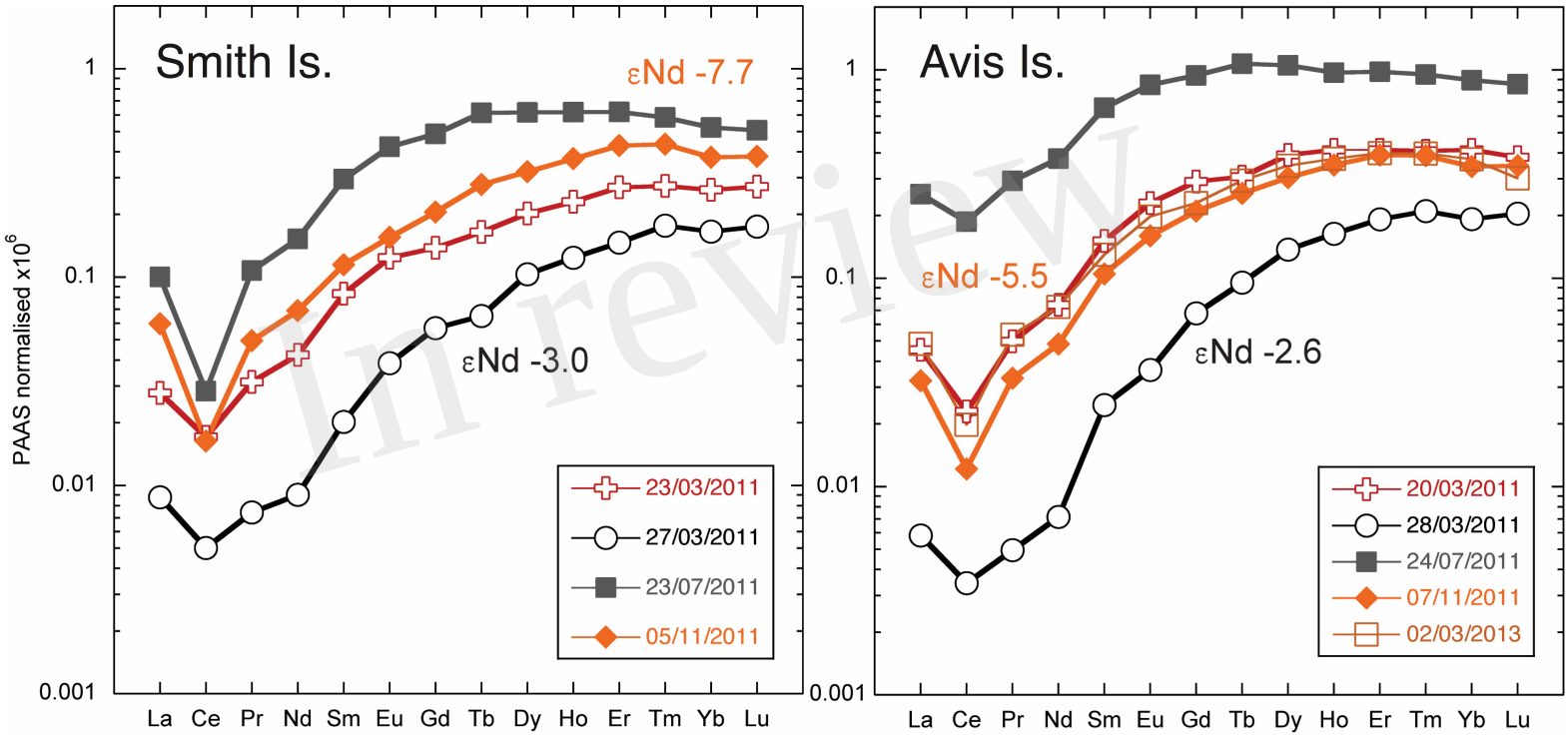

Figure 7.JPEG

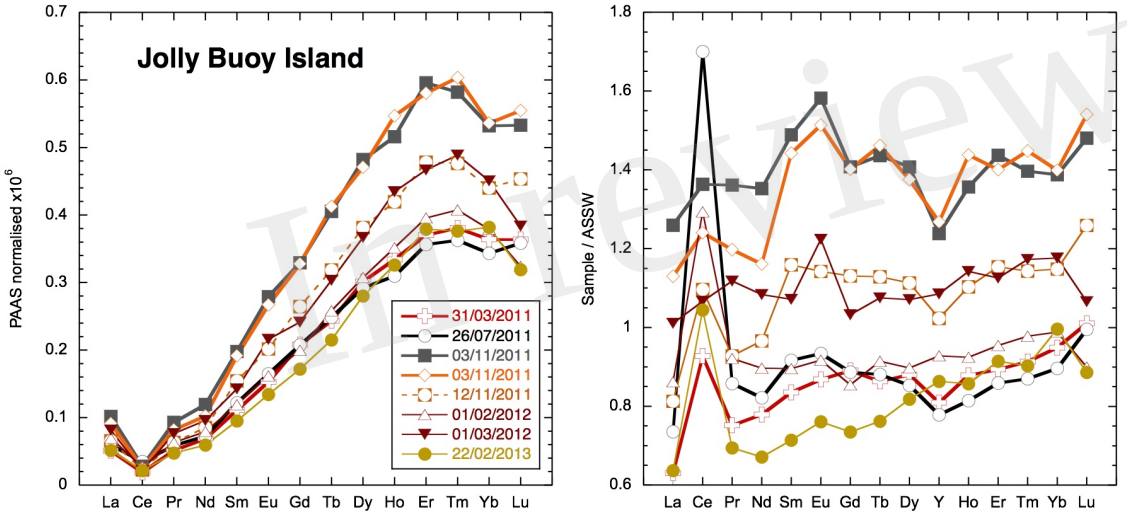

Figure 8.JPEG

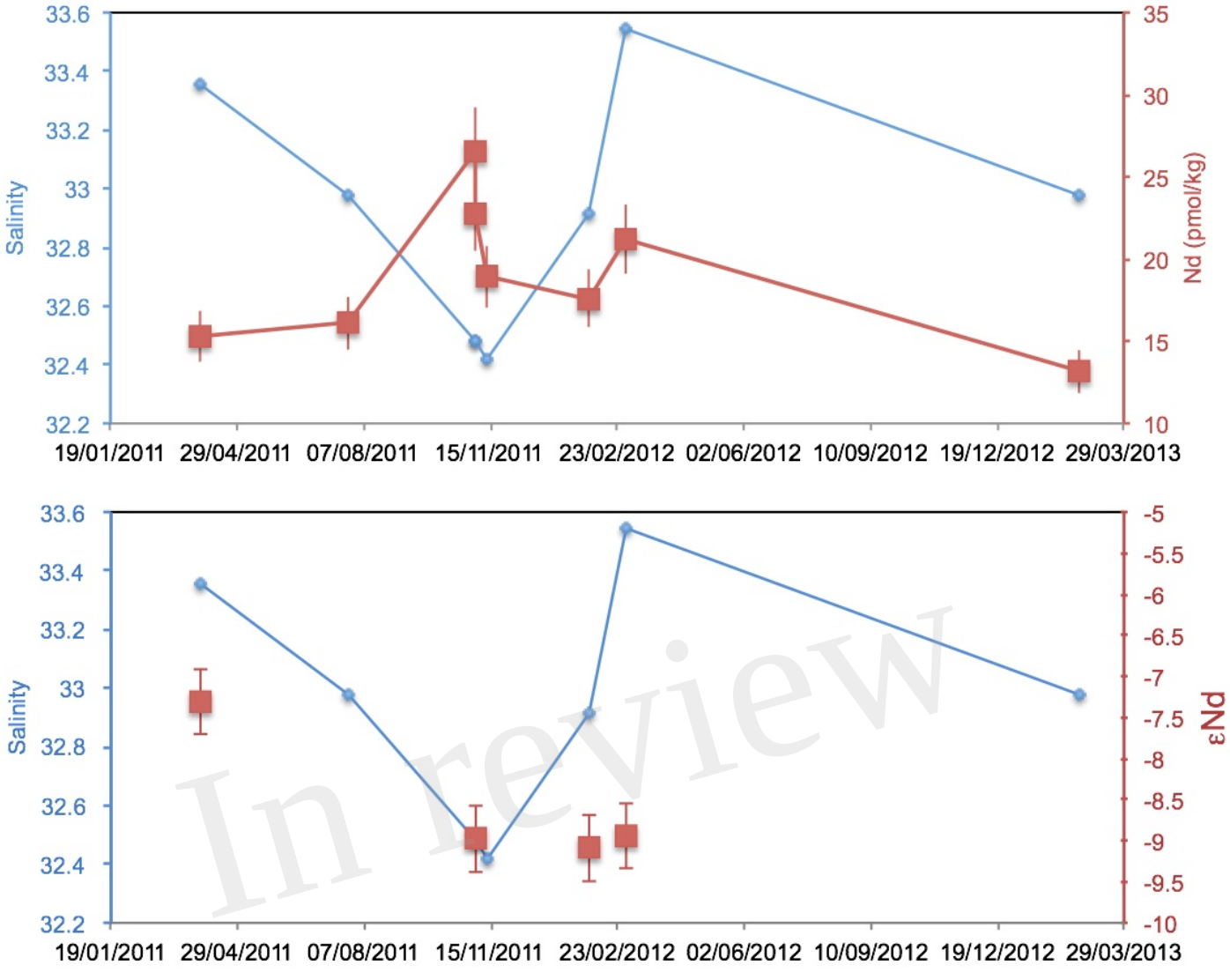

Figure 9.JPEG

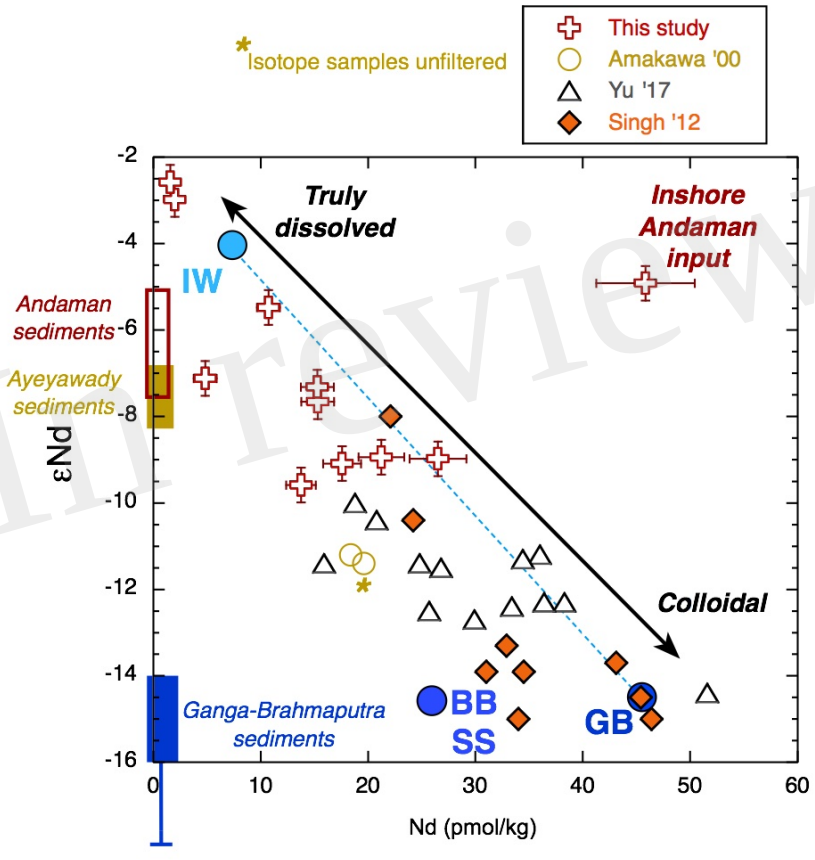

Figure 10.JPEG

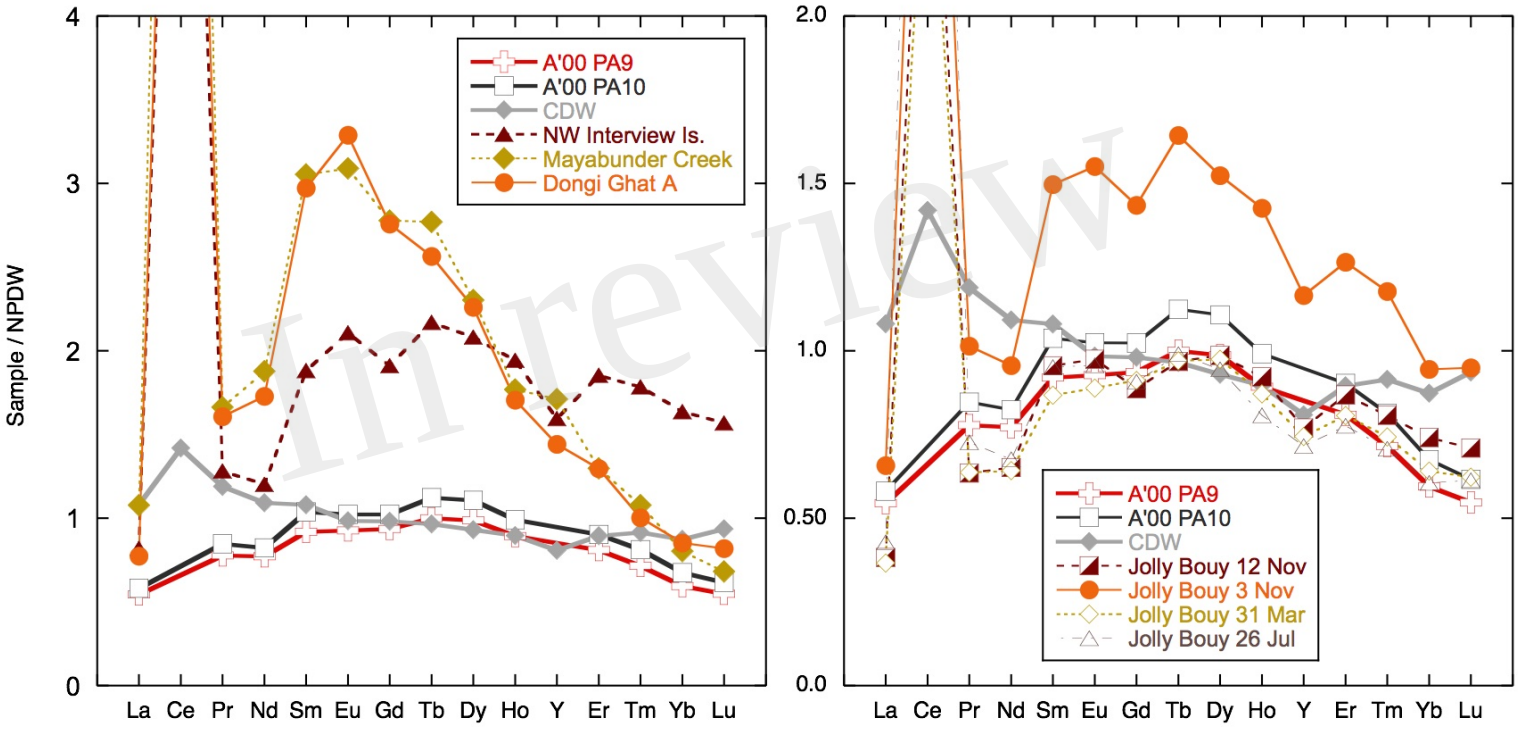

Figure 11.JPEG

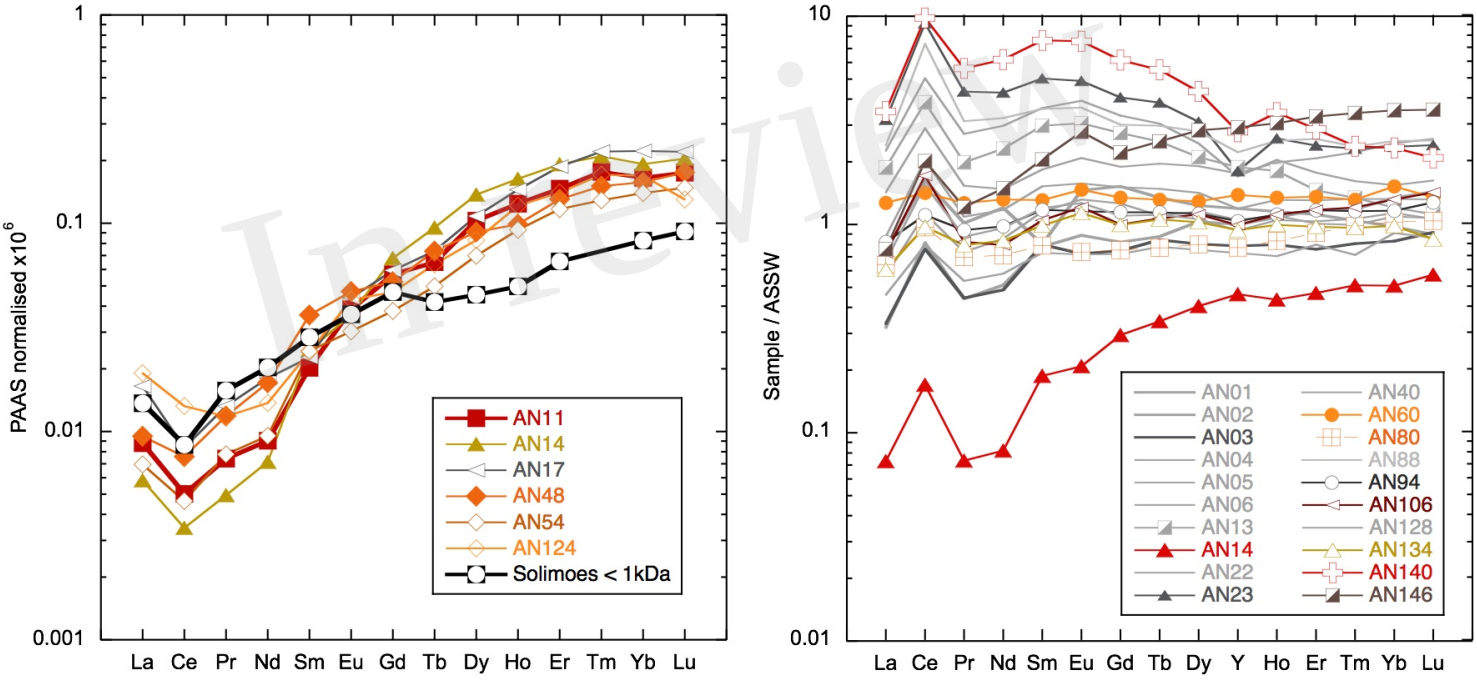

Figure 12.JPEG

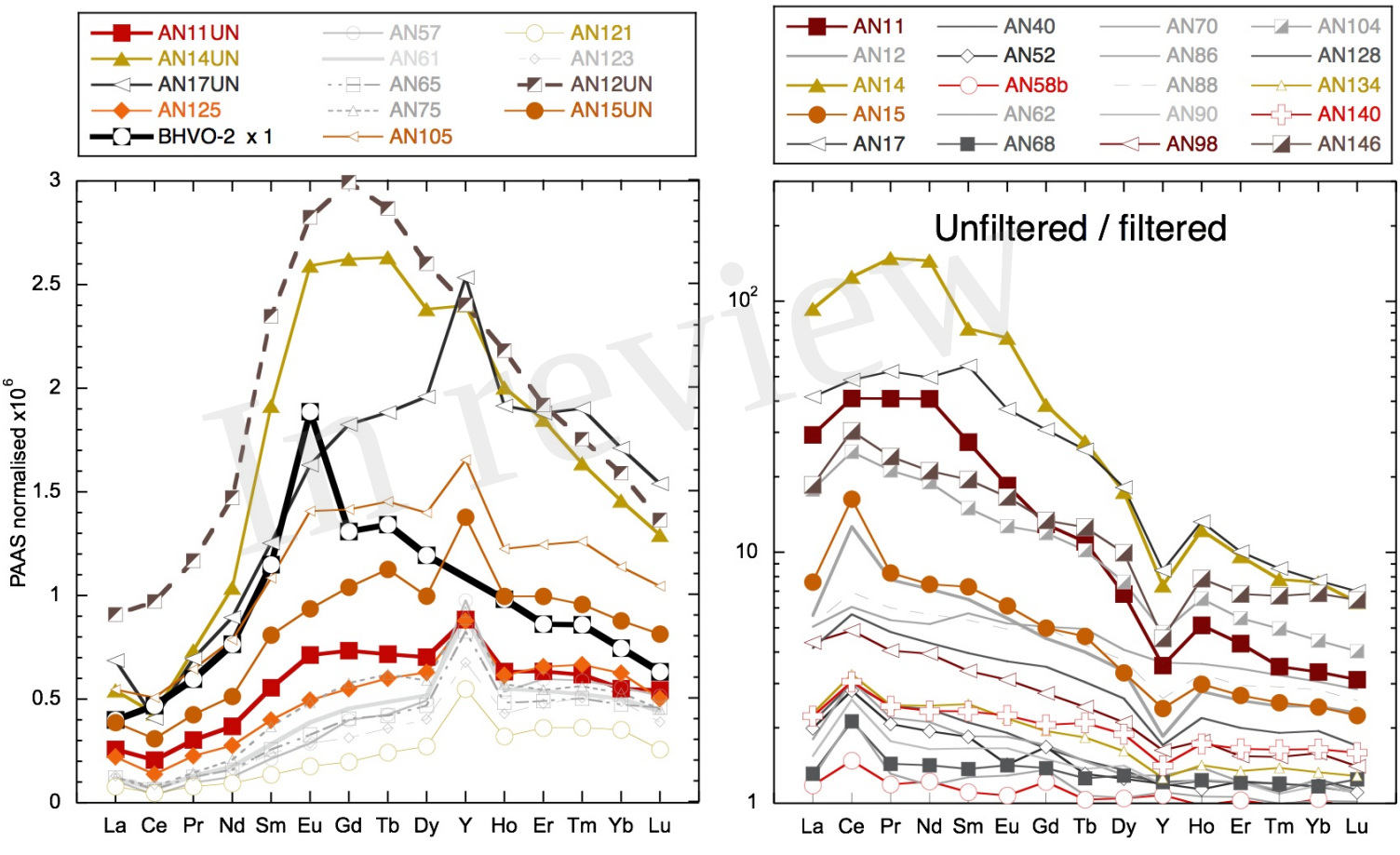

Figure 13.JPEG